

**SYNTHESIS OF POLY(VINYLPYRROLIDONE) (PVP)
GRAFTED SILICA AS MATRIX FOR GENERATION OF
PALLADIUM NANOPARTICLES AND INVESTIGATION
OF EFFECT OF GRAFT LENGTHS ON CATALYTIC
ACTIVITY**

**PALADYUM NANOPARÇACIKLARIN ÜRETİMİ İÇİN
MATRİS OLARAK POLİ(VİNİLPİROLİDON) (PVP)
AŞILANMIŞ SİLİKA SENTEZİ VE AŞI UZUNLUKLARININ
KATALİTİK AKTİVİTEYE ETKİSİNİN ARAŞTIRILMASI**

TANSU ÇAYLAN

DOÇ. DR MURAT BARSBAY

Supervisor

Submitted to

Graduate School of Science and Engineering of Hacettepe University

as a Partial Fulfillment to the Requirements

for the Award of the Degree of Master of Polymer Science and Technology.

2019

This work titled “**Synthesis of Poly(vinylpyrrolidone) (PVP) Grafted Silica as Matrix for Generation of Palladium Nanoparticles and Investigation of Effect of Graft Lengths on Catalytic Activity**” by TANSU ÇAYLAN has been approved as a thesis for the **Degree of MASTER OF POLYMER SCIENCE AND TECHNOLOGY** by the Examining Committee Members mentioned below.

Prof. Dr. Murat ŞEN

Head



Assoc. Prof. Dr. Murat BARSBAY

Supervisor



Prof. Dr. Hatice KAPLAN CAN

Member



Assoc. Prof. Dr. Esra BAĞDA

Member



Assist. Prof. Dr. Meshude AKBULUT SÖYLEMEZ

Member



This thesis has been approved as a thesis for the **Master in POLYMER SCIENCE AND TECHNOLOGY** by Board of Directors of the Institute for Graduate School of Science and Engineering on/...../.....

Prof. Dr. Menemşe GÜMÜŞDERELİOĞLU

Director of the Institute of

Graduate School of Science and Engineering

To my lovely husband and previous family...

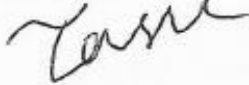
ETHICS

In this thesis study, prepared in accordance with the spelling rules of Institute of Graduate School of Science and Engineering of Hacettepe University,

I declare that

- all the information and documents have been obtained in the base of the academic rules,
- all audio-visual and written information and results have been presented according to the rules of scientific ethics,
- in case of using other Works, related studies have been cited in accordance with the scientific standards,
- all cited studies have been fully referenced,
- I did not do any distortion in the data set,
- and any part of this thesis has not been presented as another thesis study at this or any other university.

13 / 09 /2019



TANSU ÇAYLAN

YAYINLANMA FİKRİ MÜLKİYET HAKLARI BEYANI

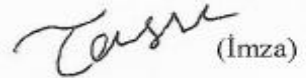
Enstitü tarafından onaylanan lisansüstü tezimin/raporumun tamamını veya herhangi bir kısmını, basılı (kağıt) ve elektronik formatta arşivleme ve aşağıda verilen koşullarla kullanıma açma iznini Hacettepe üniversitesine verdiğimi bildiririm. Bu izinle Üniversiteye verilen kullanım hakları dışındaki tüm fikri mülkiyet haklarım bende kalacak, tezimin tamamının ya da bir bölümünün gelecekteki çalışmalarda (makale, kitap, lisans ve patent vb.) kullanım hakları bana ait olacaktır.

Tezin kendi orijinal çalışmam olduğunu, başkalarının haklarını ihlal etmediğimi ve tezimin tek yetkili sahibi olduğumu beyan ve taahhüt ederim. Tezimde yer alan telif hakkı bulunan ve sahiplerinden yazılı izin alınarak kullanması zorunlu metinlerin yazılı izin alarak kullandığımı ve istenildiğinde suretlerini Üniversiteye teslim etmeyi taahhüt ederim.

Yükseköğretim Kurulu tarafından yayınlanan “*Lisansüstü Tezlerin Elektronik Ortamda Toplanması, Düzenlenmesi ve Erişime Açılmasına İlişkin Yönerge*” kapsamında tezim aşağıda belirtilen koşullar haricince YÖK Ulusal Tez Merkezi / H. Ü. Kütüphaneleri Açık Erişim Sisteminde erişime açılır.

- Enstitü / Fakülte yönetim kurulu kararı ile tezimin erişime açılması mezuniyet tarihimden itibaren 2 yıl ertelenmiştir.
- Enstitü / Fakülte yönetim kurulu gerekçeli kararı ile tezimin erişime açılması mezuniyet tarihimden itibaren ay ertelenmiştir.
- Tezim ile ilgili gizlilik kararı verilmiştir.

13 / 09 / 2019

 (İmza)

TANSU ÇAYLAN

ABSTRACT

SYNTHESIS OF POLY(VINYLPYRROLIDONE) (PVP) GRAFTED SILICA AS MATRIX FOR GENERATION OF PALLADIUM NANOPARTICLES AND INVESTIGATION OF EFFECT OF GRAFT LENGTHS ON CATALYTIC ACTIVITY

Tansu ÇAYLAN

Master of Science, Department of Polymer Science and Technology

Supervisor: Doç. Dr. Murat BARSBAY

September 2019, 73 pages

The rationale of M.S thesis work is to investigate the effect of chain length of the stabilizing polymer brushes attached to silica surface on the formation of metallic palladium nanoparticles (NPs) and their catalytic activity. Poly(vinyl pyrrolidone) (PVP) brushes forming a very thin shell was grafted from silica microparticles (Si@PVP) via RAFT mediated graft polymerization method thus controlling the molecular weights and structures of PVP grafts. Palladium (Pd) nanoparticles were formed in PVP stabilizing matrix by gamma radiolysis of Pd(II) ions to yield Pd(0) decorated core-shell particles (Si@PVP-PdNP). Size Exclusion Chromatography (SEC) and Thermogravimetric Analysis (TGA) results indicated the formation of PVP brushes with different molecular weights on silica. Dynamic Light Scattering (DLS) and Transmission Electron Microscopy (TEM) measurements revealed that increased molecular weight of PVP brushes sterically blocked the particle growth and yielded more small Pd nanoparticles rather than fewer large ones. Si@PVP-PdNP having different PVP lengths and Pd sizes were evaluated for

their catalytic activity and reusability in the model reduction of 4-nitrophenol to 4-aminophenol. It has been found that longer grafts are more effective in preventing NPs from leaking into the solution through the PVP shell, even if nanoparticles (NPs) are smaller in their presence, yet they allow the diffusion of reactants, resulting in more stable catalytic activity in repeated measurement cycles. On the other hand, short grafts are not sufficiently effective in preventing NP agglomeration and leakage. These findings are particularly important for heterogeneous catalyst systems in that they show the effects of surface-bound polymeric stabilizers on NP formation and catalytic activity.

Keywords: Surface modification, Silica micro-particles, RAFT polymerization, Palladium nanoparticles.

ÖZET

PALADYUM NANOPARÇACIKLARIN ÜRETİMİ İÇİN MATRİS OLARAK POLİ(VİNİLPİROLİDON) (PVP) AŞILANMIŞ SİLİKA SENTEZİ VE AŞI UZUNLUKLARININ KATALİTİK AKTİVİTEYE ETKİSİNİN ARAŞTIRILMASI

Tansu ÇAYLAN

Yüksek Lisans, Polimer Bilimi ve Teknolojisi Bölümü

Tez Danışmanı: Doç. Dr. Murat BARSBAY

Eylül 2019, 73 sayfa

Bu tez çalışmanın amacı, silika yüzeyine bağlı stabilize edici polimer fırçaların zincir uzunluğunun, metalik paladyum nanopartiküllerinin (NP'ler) oluşumu ve katalitik aktivitesi üzerindeki etkisini araştırmaktır. Çok ince bir kabuk oluşturan poli(vinil pirolidon) (PVP) fırçalar, silika mikropartiküllerinden Tersinir Eklenme Parçalanma Zincir Transferi (RAFT) aracılı aşı polimerizasyonu yöntemiyle aşılınmış (Si@PVP), böylece PVP aşılının moleküler ağırlıkları ve yapıları kontrol edilmiştir. PVP stabilize edici matris içinde paladyum Pd(II) iyonlarının gamma radyolizi ile metalik Pd(0)'a indirgenmesi sayesinde, Pd nanoparçacıkları ile dekore edilmiş çekirdek-kabuk formunda parçacıklar (Si@PVP-PdNP) elde edilmiştir. Büyüklükçe Ayırma Kromatografisi (BAK) ve Termogravimetrik Analiz (TGA) sonuçları silika üzerinde farklı molekül ağırlıklarına sahip PVP fırçalarının oluştuğuna yönelik sonuçlar vermiştir. Dinamik Işık Saçılımı (DLS) ve Geçirimli Elektron Mikroskopisi (TEM) ölçümleri, artan PVP aşı uzunluklarının, Pd nanoparçacıklarının büyümesini sterik olarak engelleyerek daha fazla sayıda küçük Pd nanoparçacıklarının oluşumuna sebep olduğunu göstermiştir.

Farklı PVP uzunluklarına ve Pd nanoparçacık boyutlarına sahip olan Si@PVP-PdNP örnekleri, model olarak seçilen 4-nitrofenol'ün 4-aminofenol'e indirgenme reaksiyonunda katalitik aktiviteleri ve yeniden kullanılabilirlikleri açısından değerlendirilmiştir. Yüksek mol kütleli polimer zincirlerinin aşılandığı yapılarda daha küçük nanoparçacıklar oluşsa da, uzun aşılı zincirlerinin bu nanoparçacıkların çözeltiye sızmalarını sterik olarak önlemede daha etkili oldukları, ancak yine de reaktiflerin difüzyonuna izin vermeleri sayesinde tekrarlanan ölçüm döngülerinde daha kararlı aktivite sağladıkları görülmüştür. Öte yandan, kısa aşılı zincirlerinin nanoparçacıkların aglomerasyonunu ve sızıntısını önlemede yeterince etkili olmadıkları ortaya konmuştur. Bu bulgular, yüzeye bağlı polimerik stabilizatörlerin, özellikle heterojen katalizör sistemlerinde kullanımlarında, nanoparçacık oluşumu ve katalitik aktivite üzerinde etkilerini göstermeleri bakımından önemlidir.

Anahtar Sözcükler: Yüzey modifikasyonu, Silika mikro-parçacıklar, RAFT polimerizasyonu, Paladyum nanoparçacıklar.

ACKNOWLEDGEMENTS

Foremost, with profound respect and esteemed consideration, I would like to thank my supervisor Doç. Dr. Murat BARSBAY, who guides me throughout my MSc study at every stage. I am deeply grateful to him for his patience, motivation, support, and extensive knowledge. It is an honor to study with him.

I would also like to thank Dr. Semiha Duygu SÜTEKİN for all of her support and for sharing her invaluable knowledge. I thank to Dr. Anastassiya A. Mashentseva for her assistance in catalytic activity measurement tests. Also, I would like to thank all the other labmates who did not spare their support.

I also wish to express sincere thanks to Volkan for all of his moral support.

I am thankful to my husband Ahmet who made sense of my life with love for his support, understanding and endless patience at home. Without his love and support everything would have been more difficult, thank you very much true person.

Finally, the most important part of my life is my family. I would like to express my special thanks to my beloved family; my mother, Gönül, my father, Sami and especially my twins, Cansu, for their guidance, unending inspiration and morale support during my thesis. I am so lucky to have them.

I acknowledge that this study was supported by IAEA Coordinated Research Project F22070, entitled ‘Enhancing the Beneficial Effects of Radiation Processing in Nanotechnology’.

TABLE OF CONTENTS

| | |
|--|------|
| ABSTRACT | i |
| ÖZET | iii |
| ACKNOWLEDGEMENTS | v |
| TABLE OF CONTENTS | vi |
| FIGURES | viii |
| LIST OF TABLES | xi |
| LIST OF ABBREVIATIONS | xii |
| 1. INTRODUCTION | 1 |
| 2. GENERAL INFORMATION | 4 |
| 2.1. Surface Modification | 4 |
| 2.1.1. Graft Polymerization | 5 |
| 2.1.1.1. Surface Functionalization in a Controlled-manner | 7 |
| 2.2. Controlled/living Radical Polymerization (CRP) Techniques | 8 |
| 2.2.1. Atom Transfer Radical Polymerization (ATRP) | 11 |
| 2.2.2. Nitroxide-Mediated Polymerization (NMP) | 13 |
| 2.2.3. Reversible Addition-Fragmentation Chain Transfer Polymerization (RAFT) | 15 |
| 2.3. Surface Functionalization via RAFT Mediated Graft Polymerization and Stabilizing Effect of Surface-attached Grafts | 19 |
| 2.4. Metal Nanoparticles and Their Stabilization | 20 |
| 2.5. Preparation of Metal Nanoparticles by Ionizing Radiation | 22 |
| 2.5.1. The Effect of Radiation Dose Rate and Absorbed Dose | 25 |
| 3. EXPERIMENTAL | 26 |
| 3.1. Materials | 26 |
| 3.2. Attenuated Total Reflectance Fourier Transform Infra-Red (ATR-FTIR) Spectroscopy | 26 |
| 3.3. X-Ray Photoelectron Spectroscopy (XPS) | 26 |
| 3.4. UV-Vis Spectroscopy | 26 |

| | |
|---|----|
| 3.5. Dynamic Light-Scattering (DLS)..... | 27 |
| 3.6. Atomic Force Microscopy (AFM) | 27 |
| 3.7. Scanning Electron Microscopy (SEM) Imaging and Energy Dispersive X-Ray (EDX) Mapping..... | 27 |
| 3.8. Transmission Electron Microscopy (TEM) | 27 |
| 3.9. Size Exclusion Chromatography (SEC) Analysis | 27 |
| 3.10. Thermogravimetric Analysis (TGA) | 28 |
| 3.11. Synthesis of 4,4'-Azobis(4-cyanopentanoic acid) (ACPA) Functionalized Silica (Si@ACPA) | 28 |
| 3.12. Synthesis of Poly(vinylpyrrolidone) (PVP) Grafted Silica Micro-particles (Si@PVP)..... | 28 |
| 3.13. Formation of Palladium Nanoparticles Stabilized by PVP (Si@PVP-PdNP):..... | 29 |
| 3.14. Catalytic Activity Measurements | 29 |
| 4. RESULT AND DISCUSSION | 31 |
| 5. CONCLUSION | 52 |
| REFERENCES | 54 |
| CURRICULUM VITAE | 71 |

FIGURES

| | |
|--|----|
| Figure 2.1. Techniques of "grafting to", "grafting through" and "grafting from"[45]. | 6 |
| Figure 2.2. A general controlled radical polymerization mechanism [54]. | 10 |
| Figure 2.3. Various polymer architectures prepared using CRP [69]. | 11 |
| Figure 2.4. Schematic representation of the ATRP process [73]. | 12 |
| Figure 2.5. The activation-deactivation mechanism in NMP [83]. | 14 |
| Figure 2.6. Mechanism for reversible addition-fragmentation chain transfer (RAFT) polymerization [95]. | 16 |
| Figure 2.7. Comparison of polymers made with traditional radical polymerization and RAFT process [103]. | 17 |
| Figure 2.8. General structures of different classes of thiocarbonylthio RAFT agents [105]. | 18 |
| Figure 2.9. Representation of PVP coated silica microparticles with stabilized metal nanoparticles. | 20 |
| Figure 2.11. The electromagnetic spectrum illustrating the range of frequencies of all radiation. | 23 |
| Figure 2.12. The effect of dose rate on the size of nanoclusters generated [4]. | 25 |
| Figure 4.1. GPC chromatograms as a function of (a) polymerization time, (b) VP/RA1 molar ratio. (c) Experimental and theoretical number-average of molecular weights as a function of monomer conversion and PD values obtained by using VP/RA1: 452 molar ratio. | 33 |
| Figure 4.2. TGA thermograms of (a) initiator-immobilized silica (Si@ACPA), PVP and PVP grafted silica (Si@PVP) samples with different polymerization time, (b) Si@NH ₂ , ACPA and Si@ACPA, (c) Si@PVP samples with different target molecular weights. Target chain length was derivatized by changing the [VP]/[RA1] molar ratio. | 34 |
| Figure 4.3. FTIR spectra of initiator-immobilized silica (Si@ACPA) and PVP grafted silica (Si@PVP) samples. | 36 |
| Figure 4.4. Composition of FTIR spectrum of Si@NH ₂ and Si@ACPA. The carbonyl (C=O) peak of ACPA appears at 1621 cm ⁻¹ . | 36 |

| | |
|---|----|
| Figure 4.5. SEM images of (a) Si@NH ₂ , (b) Si@ACPA and (c) Si@PVP50-8h | 37 |
| Figure 4.6. SEM images of (a) Si@NH ₂ , (b) Si@ACPA and (c) Si@PVP84-8h and corresponding SEM-EDX mappings for Si (indicated by «1», blue) and for N (indicated by «2», red) atoms. | 38 |
| Figure 4.7. Survey wide-scan XPS spectra of (a) Si@NH ₂ , (b) Si@ACPA, (c) Si@PVP20-8h and (d) Si@PVP84-8h. | 39 |
| Figure 4.8. C1s spectra of (a) Si@NH ₂ , (b) Si@ACPA and (c) comparison of C1s spectra of various samples..... | 40 |
| Figure 4.9. UV-vis absorption spectra of Pd(OAc) _{2(aq)} and filtrates of Si@PVP-Pd NP samples prepared in different solvents. | 41 |
| Figure 4.10. (a) DLS distribution of filtrates of Si@PVP50-PdNP prepared in ethanol (green), %40 EtOH/water (red), water (blue) and non-irradiated Pd(OAc) ₂ solution in %40 EtOH/water (black). (b) DLS distribution of Si@PVP50-PdNP prepared with VP: Pd ratio as 1:1 (blue) and 1:10 (red)..... | 43 |
| Figure 4.11. (a) AFM height and (b) phase images of Si@PVP50-PdNP: Irradiation dose: 10 kGy, 0.45 Mm Pd(OAc) ₂ precursor solution in EtOH:water mixture (40:60, v/v). | 44 |
| Figure 4.12. (a) Survey wide XPS scans and (b) Pd 3d core level scans of Pd(OAc) ₂ absorbed PdSi@PVP50 sample before and after irradiation. | 46 |
| Figure 4.13. DLS distribution of Pd(OAc) ₂ and filtrates of Si@PVP-PdNP samples with different PVP lengths following the irradiation (10 kGy, solvent:EtOH:water (40:60, v/v), Pd:VP=1:10) | 47 |
| Figure 4.14. TEM images of Si@PVP20-PdNP (a, zoomed in b), Si@PVP50-PdNP (c) and Si@PVP84-PdNP (d)..... | 48 |
| Figure 4.15. (a) TEM image of Si@PVP50-PdNP and (b) corresponding EDX mapping analysis for Pd element. Green arrows point small individual Pd seeds while yellow arrows show to denser areas where bigger particles are formed either by seed growth or aggregation. | 49 |
| Figure 4.16. Time dependent UV-Vis absorption spectra for the reduction of 4-NP by NaBH ₄ in the presence of (a) Si@PVP20-PdNP and (b) Si@PVP84-PdNP. Plot of ln(A _t /A ₀) vs time (c) for the reduction of 4-NP by NaBH ₄ in the presence of Si-PVP20@PdNP (■) and PVP84@PdNP (●)..... | 50 |

Figure 4.17. Catalytic performance in terms of ratio of reduced 4-NP obtained in the successive catalytic runs after isolation and redispersion of (a) Si@PVP84-PdNP, and (b) Si@PVP20-PdNP. $[4\text{-NP}]_0 = 3.91 \times 10^{-6}$ M, Si@PVP = 5.0 mg at 25.0 °C51

LIST OF TABLES

| | |
|---|----|
| Table 4.1. Reversible addition fragmentation chain transfer (RAFT) mediated grafting of N-vinylpyrrolidone (VP) from silica surface in water at 65 °C with RA1 as RAFT agent, [VP] = 2.53 M..... | 32 |
| Table 4.2. DLS results of non-irradiated Pd(OAc) ₂ and Si@PVP-PdNP prepared in different solvents and/or with different PVP lengths. | 42 |

LIST OF ABBREVIATIONS

Symbols

| | |
|-----------|--------------|
| eV | Electro-Volt |
| mW | Milli-Watts |
| nm | Nanometre |
| V | Volt |
| μm | Micrometre |

Abbreviations

| | |
|-------------------------|---|
| ACPA | 4,4'-Azobis(4-cyanopentanoic acid) |
| AFM | Atomic Force Microscopy |
| AIBN | Azo-bis-isobutyronitrile |
| ATR-FTIR | Attenuated Total Reflectance Fourier Transform Infra-Red Spectroscopy |
| ATRP | Atom Transfer Radical Polymerization |
| CRP | Controlled/living Radical Polymerization |
| CTA(s) | Chain Transfer Agent(s) |
| DCC | N,N' Dicyclohexyl Carbodiimide |
| DMF | Dimethylformamide |
| DLS | Dynamic Light Scattering |
| EtOH | Ethanol |
| GD | Grafting Degree |
| M | Monomer |
| MW | Molecular Weight |
| Mn | Number-average Molecular Weight |
| NaBH₄ | Sodium Borohydride |

| | |
|----------------------------|--|
| NaNO₃ | Sodium Nitrate |
| NMP | Nitroxide Mediated Polymerization |
| NP(s) | Nanoparticle(s) |
| PD | Polydispersity |
| Pd(OAc)₂ | Palladium(II) Acetate |
| RA1 | O-ethyl-S-(1-methoxycarbonyl) Ethyl Dithiocarbonate |
| 4-NP | 4-Nitrophenol |
| 4-AP | 4-Aminophenol |
| Pd | Palladium |
| PVA | Poly(vinylalcohol) |
| PVP | Poly(vinylpyrrolidone) |
| RAFT | Reversible Addition Fragmentation Chain Transfer Polymerization |
| SEC | Size Exclusion Chromatography |
| SEM | Scanning Electron Microscopy |
| Si-NH₂ | 3-Aminopropyl-Functionalized Silica |
| Si@ACPA | 4,4'-Azobis(4-cyanopentanoic acid) Functionalized Si-NH ₂ |
| Si@PVP | Poly(vinylpyrrolidone) Grafted Silica Micro-particles |
| Si@PVP-PdNP | Palladium Nanoparticle Decorated Si@PVP |
| TEM | Transmission Electron Microscopy |
| TGA | Thermogravimetric Analysis |
| VP | N-vinylpyrrolidone |
| XPS | X-ray Photoelectron Spectroscopy |

1. INTRODUCTION

In the past few decades, the development in synthesis of new materials in the nanosize region resulted in revolutionary developments in science and engineering as these materials present unique properties that are significantly different from those of their bulk counterparts. Metal nanoparticles are one of the most versatile and promising ones among the nanosized materials and can be used in many applications such as catalysts, medicine, microelectronics, etc. [1]. Metal nanoparticles have been widely investigated due to their enhanced reactivity by virtue of their intrinsic electronic and surface properties and high surface area to volume ratio [2, 3].

Metal colloids are generally prepared via the reduction of precursor metal ions in solution in the presence of a stabilizing agent [3]. Irradiation, using of chemical reducing agents and thermolysis are among the most commonly used techniques [2, 4]. High reproducibility and mild reaction conditions such as ambient temperature and pressure are among the biggest advantages of radiolytic synthesis compared to other available methods. Furthermore, hydrated electrons which are the main reducing agents formed during the radiolysis process in the absence of oxygen enable any metal ions to be reduced to zero-valent metal atoms. Under irradiation, the production of primary atoms occurs independently and homogeneously as each ionic precursor is distributed uniformly and reduced individually. This along with the elimination of excess chemical reducing agents leads to the formation of highly stable and homogeneously dispersed nanoparticles. Therefore, radiolytic synthesis of metallic nanoclusters has been attributed as an environmentally benign and low-cost method for controlling the size and structure of metal nanoparticles by precise tuning of nucleation and growth steps [5–7].

High reactivity of metal nanoparticles derives from active metal atoms on the surface which possess high catalytic activity. However, particle stability against agglomeration should be ensured by using suitable supports and stabilizers. Polymers having functional groups such as $-\text{NH}_2$, $-\text{COOH}$ and $-\text{OH}$ are commonly used as stabilizing materials for many noble metals such as Au, Ag, Pt, and, of interest to this study, Pd. Palladium

nanoparticles have been widely exploited as recyclable and highly active catalysts in many industrial applications due to their high activity in organic reactions such as Suzuki, Heck, and Stille couplings [8, 9]. However, Pd nanoparticles have a high tendency to aggregation to form palladium black which results in an increase in particle size and instability and eventually, considerable loss of catalytic activity [10]. To enhance the stability of Pd nanoparticles (NPs), polymeric support materials are mostly needed. In this work, poly(vinylpyrrolidone) (PVP) has been selected as the stabilizing matrix since it was reported as the polymer with the highest stabilizing effect on many metallic NPs in comparison with other widely used stabilizers such as poly(acrylic acid) or poly(N-vinylimidazole) [11].

In an industrial point of view catalysts should possess not only selectivity and high activity but they also have to be cost-effective, stable, easily accessible and recyclable. Therefore, solid state heterogeneous catalyst systems are preferred in accordance with the requirements for industrial applications. Silica is an important solid support for heterogeneous catalysts systems because of its abundant availability, high stability and ease of modification of its surface. Surface modification by using functional group immobilization ensures unique chance to tailor the interfacial properties of solid substrates. It has been shown that by placing functional groups on silica, Pd nanoparticles are more effectively stabilized and their recovery is increased [12–14]. Surface grafting is a versatile method allowing covalent attachment of desired macromolecular chains on various polymeric surfaces, membranes, silica, metals, nano tubes, etc. and it ensures long-term chemical stability of the surface which cannot be attained by many other surface modification methods [15].

The catalytic properties of metal NPs are commonly regarded as size- and shape-dependent [16]. However, the characteristics of the stabilizing matrix on which the NPs adsorbed also play a crucial role in their catalytic properties [17, 18]. Therefore, establishment of a method yielding tailor-made and well-defined characteristics over the stabilizing matrix is one of the key points to attain high and reproducible catalytic activity. In recent years a great deal of research has been made to carry out surface modifications in a controlled manner due to the fact that molecular weight, polydispersity, functionality, chain structures and compositions of polymers which are of paramount importance for a

diversity of applications can only be adjusted through controlled polymerization techniques. The reversible addition-fragmentation chain transfer (RAFT) polymerization is regarded as the most versatile and effective mechanism among the other controlled polymerization methods in tailoring the characteristics of the polymer chains. This method is suitable for a wide range of monomers, solvents and initiators, and predictable molecular weights and low polydispersities can be attained via this polymerization technique [19–24]. Various polymers serving as stabilizing matrixes have been widely used in chemical synthesis of metal nanoparticles. However, the role of their molecular weight has been rarely concerned. Song et al. exhibited that the molecular weight of stabilizing polymer plays a critical role in the shape control of metal nanoparticles (e.g. nanospheres, nanowires) as a result of differences in adsorption effects and steric hindrances [25]. The average size of Pd nanoparticles reportedly increases with increasing molecular weight of the stabilizing polymer dissolved in solution [26]. Shimmin et al., on the other hand, found that average particle size decreases with increasing polymer molecular weight due to polymer's steric bulk in blocking particle growth [27]. These contradictory studies examine the relation between the molecular weight of soluble, i.e. free, stabilizing polymer in solution and nanoparticle size. To the best of our knowledge, no study has been published on the relationship between the nanoparticle size and molecular weight of the polymer chains grafted on a substrate potential to be used as a heterogeneous solid catalyst system. In the present thesis, we varied the molecular weights of PVP grafts on silica via RAFT polymerization and found out that lengths of the grafted chains are an assistant factor to control the size and seed growth process of the synthesized nanoparticles.

2. GENERAL INFORMATION

2.1. Surface Modification

Polymeric materials are used successfully in many different fields such as biomaterials, electronic devices, packaging, coating, protective materials, composite and catalytic applications [28]. In order to use these applications, some special properties such as hydrophilicity, ionic charge, molecular adsorption, molecular permeability, roughness must be acquired in addition to the chemical structures of the material [29]. Polymers generally do not have these desirable properties in their compositions for these applications. Therefore, by using surface modification techniques, valuable modified products can be obtained.

Surface modification is defined as modifying surface of a material by providing physical, chemical and biological changes, and the resulting product is different from the original material surface. Some changes can be made on the surface with surface modification without affecting their bulk characteristics. Surface modification by using functional group immobilization ensures unique chance to engineer the interfacial properties of solid substrates. When selecting the surface modification technique to be used, the compatibility of the polymers with the prepared surface and their formation under different reaction conditions should be noted. A detailed description of polymer surface modification techniques can be categorized into three broad groups:

- physicochemical-based surface modifications based on covalently attaching new compositions (molecules/elements/ions) on existing surfaces to produce new polymer surface (e.g., UV-irradiation, self-assembly, grafting, coating, etching, layer by-layer and Langmuir-Blodgett techniques) [30]
- mechanical-based surface modifications based on mechanical processing (in the absence of chemicals) to modify the surface chemistry (e.g., roughening, micromanipulation) [31]
- biological-based surface modifications based on biologically attachment to existing surfaces to immobilize biomolecules and cells (e.g., physical adsorption, physical entrapment and chemical or covalent attachment)

These sub-categories such as blending, coating, grafting, abrasive blasting, roughening and curing result in producing new surface composition with desired properties [32]. This work will promote surface grafting as a sub-category method of surface modification to improve the properties of materials. Grafting method provides connection between two monomers through covalent bonding, whereas polymerization is defined as forming polymer chains or three dimensional networks by reacting monomer molecules covalently. Thus, combination of both grafting and polymerization is an attractive and effective method to bond various functional groups on the polymer and improve its bulk properties [33].

2.1.1. Graft Polymerization

Surface grafting is defined as the introduction of a polymer chain to the surface of a substrate such as another polymer or an organic/inorganic material and many of the surface properties can be altered by this method. A thin film can be obtained on the surface of various substrates by some techniques such as spin casting, precipitation, polymer adsorption, etc. [32]. However, among all these techniques, the significance of chemical grafting is greater than others as it is an extremely versatile in terms of providing remarkable properties such as high surface density, exact localization and stable grafted structures on the material surface in controlled and easy manner [34]. Graft polymerization provides the covalent attachment of a new polymer to an existing polymer surface, and various functional groups such as carboxyl, hydroxyl, amine, halogens and organosilane groups can be introduced to the structure [35]. The grafting method is irreversible due to covalent attachment to the structure. The grafting of polymer brushes to surface leads to a versatile tool for surface modification and functionalization. Controlled-living radical polymerization techniques may also employed during the graft polymerization technique [36–43]. By combination of these techniques with graft polymerization, various surfaces can be modified by polydispersity polymers with the high graft density [44].

In general, three approaches; the ‘grafting to’, ‘grafting through’ and ‘grafting from’ processes can be used for bonding of a polymer chain covalently onto a surface [45] as can be expressed in Figure 2.1.

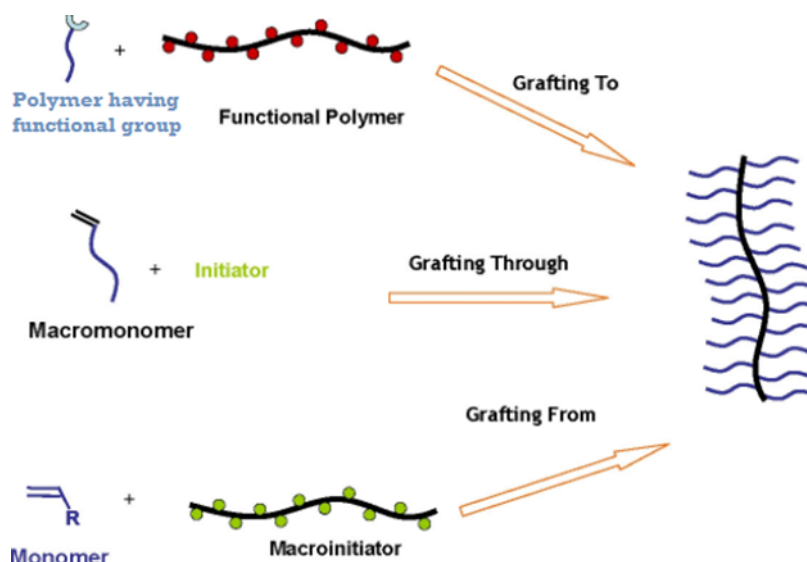


Figure 2.1. Techniques of "grafting to", "grafting though" and "grafting from"[45].

'Grafting to' approach

The 'grafting to' technique is carried out by reaction between the end-group functionalized polymers and supplementary functional groups on the surface, which leads to formation of the tethered chains at the end of the reaction. The polymers can be obtained by conventional, controlled radical, living and other polymerization techniques. The main benefit of the 'grafting to' method over the other polymerization techniques is characterization of polymer via physical and chemical methods before the grafting. In addition, this grafting method does not require very complex synthesis reactions, and in general it is a less compelling method. Nevertheless, an important lack of this technique is that maximum thickness of the layers is low [46]. When the amount of grafted chains increase in the 'grafting to' method, the new chains may not reach the surface and polymer chains may not be able to tether to the solid surface adequately. Since the polymer chains cannot diffuse to the existing surface of the solid, 'grafting to' method is defined as self-limiting process [47].

'Grafting from' approach

In the 'grafting from' method, the growth of the chains is provided from out of the surface by the help of initiator groups. Proper initiator group is covalently connected to the solid surface depending on polymerization mechanism chosen for grafting. With this method, grafted polymeric structures with high chain density and high mass per unit area are

obtained and it is easy for monomer molecules to penetrate these structures [48]. Furthermore, this method has demonstrated its impact in preparation thick layers with high-density polymer on the solid surface [49].

'Grafting through' approach

The other approach is 'grafting through' also known as a macro-monomer method. In this method polymerization of the chain end groups which are present in pre-synthesized macro-monomer structures is carried out. First, in this method, polymerizable groups at the chain ends are polymerized and then molecular brushes are obtained as a result of these polymerized structures [50]. After the appropriate polymerization technique is selected, side chains can be synthesized and the desired and controllable cylindrical polymer brushes can be achieved. The grafting density of each monomeric structure can also be controlled [51]. Nevertheless, when the published studies are examined, 'the grafting through' method has some inherent disadvantages; molecular weight control and polymerization of high molecular weight macro-monomers is poor and difficult. The conversion of the obtained macro-monomers does not take place completely [52].

It is clear from such reasons that the 'grafting from' technique seems to be preferred among the strategies to synthesize grafted molecular structures.

2.1.1.1. Surface Functionalization in a Controlled-manner

It is important to modify the surface properties of a polymer in accordance with tailor-made specifications designed for target usages. Therefore, in recent years a great deal of research has been made to carry out surface modifications under controlled polymerization conditions. Polymers produced by controlled polymerization conditions have a wide range of reasonable applications such as drug delivery, nanoparticle, bio-mineralization applications, composite, memory devices, coatings, lubricants, adhesives designing and many others [53]. In addition, the molecular weight, polydispersity indexes, functionality, chain structures and compositions of polymers can be adjusted through controlled manner.

The living ionic polymerizations are able to produce polymers with well-defined structures, such as pre-determined copolymer compositions, controlled molecular weights,

narrow molecular weight distribution, end-group functionalities, etc. However, ionic polymerizations are only applicable for a limited range of monomers and they are susceptible to moisture, many acidic or basic compounds and carbon dioxide [54]. The conventional free-radical polymerization, on the other hand, is widely used to prepare high molecular weight polymeric structures with a wide range of functional monomers. Some major advantages of free-radical polymerization technique are the relative insensitivity to impurities, its adaptability under less stringent synthesis conditions and the multiple polymerization processes present [55]. Unfortunately, some disadvantages of free radical polymerization are there is no control of the molecular weight and the molecular weight distribution, and the preparation of well-defined homo- or co- polymers with functional groups is very difficult [56].

Therefore, it has been very promising to combine the benefits of ionic and conventional free-radical polymerization techniques in one polymerization process to obtain polymeric structures having different functional structures such as block, graft copolymers, stars, brush, combs, and networks, end-functional polymers under suitable mild conditions [57]. In order to success this aim, it has been found that the use of controlled free-radical polymerization (CRP) techniques are versatile and effective either for the synthesis of homo- or co- polymers and for compounding polymers with varied solid surfaces like silica micro particles via grafting [58]. The functionalization of a surface, namely silica in this M.S. thesis, with well-defined functional polymers provides promising materials that are at the interest of polymer research.

2.2. Controlled/living Radical Polymerization (CRP) Techniques

Control over all aspects of radical polymerization was considered almost impossible since radical termination reactions occur during the conventional free-radical polymerization process. However, there are now several methods for controlling the radical polymerization. These methods are not promising only for academia; there are some companies preferring products based on CRP in many high-value markets [59]. This part briefly gives a summary of the evolution, classification, advantages and disadvantages of CRP techniques and contribution of preparation of well-defined polymers with controlled molecular weight distribution.

Controlled/Living Radical Polymerization (CRP) is among the most unprecedented opportunity in chemistry and polymer science. CRP technique is used powerfully to prepare many well-defined structures with precisely controlled structural parameters and can be used to produce materials with new special properties [60].

Conventional free-radical polymerization process has many advantages such as preparing high molecular weight polymers of many vinyl monomers, adaptability over a large temperature range (-80 to 250 °C) under very mild reaction conditions, e.g. tolerance to oxygen, etc. [61]. Unfortunately, site-specific functionality, molecular weight, molecular weight distribution (polydispersity), architecture of the polymer, and composition cannot be controlled for the macromolecular structures via this method [59]. On the other hand, transfer and termination reactions are removed in the chain growth process of ionic living polymerizations, i.e. anionic and cationic. Living polymerizations lead to control the end functional groups and the formation of block polymers. Well-defined polymeric structures with accurately controlled molecular weight and narrow molecular weight distribution are attainable by using ionic living polymerization. However, there are some drawbacks such as ionic living polymerization requires stringent conditions and are limited usage of monomers, susceptibility of carbon dioxide, moisture, some acid and basic compounds [62-64]. Therefore, it is desirable to obtain end-functional and well-defined polymers by free radical means. Synthesis of homo- or copolymers, such as block, stars, combs, and gradient copolymers under mild conditions for a large number of monomers has always been challenging in polymer science [65]. This is the main reason why we have witnessed a real historical development of 'controlled/'living' radical polymerizations (CRP) in academia and also in many new industrial application areas since the late 1990s.

The term 'controlled' has been used for systems that control molecular weight and molecular weight distribution [66]. The 'living' term refers the formation of well-defined polymers having low polydispersities under conditions when chain transfer reactions are repressed and an equilibrium between end-capped chains that are dormant and active chains is provided in a radical polymerization [67, 68]. The term 'controlled/living' could also define the unprecedented opportunity to obtain functional polymers with targeted properties. CRP can be introduced as "a radical polymerization that can be stopped and re-initiated under externally control" and the schematic representation is as follows in Figure

2.2 [54]. Equilibrium is provided between end-capped chains that are dormant, unable to propagate or terminate, and the active species. The equilibrium must be moved towards the dormant species and exchange between the two types of CRP reaction, namely active and dormant species must be fast relative to propagation. CRP techniques become more essential than conventional radical polymerization with property of having a reversible activation process.

General CRP mechanism can be shown as follows;

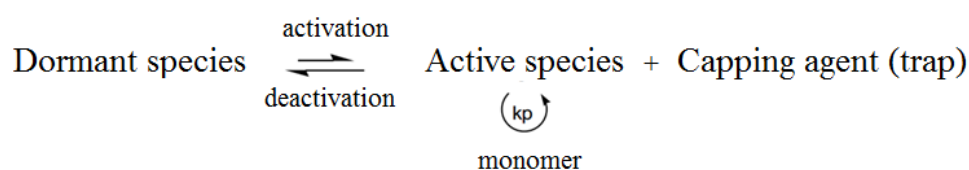


Figure 2.2. A general controlled radical polymerization mechanism [54].

A number of CRP methods have been developed and three most important methods are nitroxide mediated polymerization (NMP), atom transfer radical polymerization (ATRP) and reversible addition fragmentation chain transfer (RAFT) polymerization. A dynamic equilibrium between active propagating chains having a low concentration and a predominant amount of dormant chains that are unable to propagate or terminate is established for each of these methods to increase the lifetime of the propagating chains [59]. Homo-polymers, graft, block, random, and different molecular shapes such as linear, networks, cross-linked, branched, comb, star, brush polymer etc. have been successfully synthesized via CRP methods [54]. The success of the CRP is shown with examples of polymers with an unprecedented opportunity in materials design, different topologies, compositions and functionalization at the following Figure 2.3.

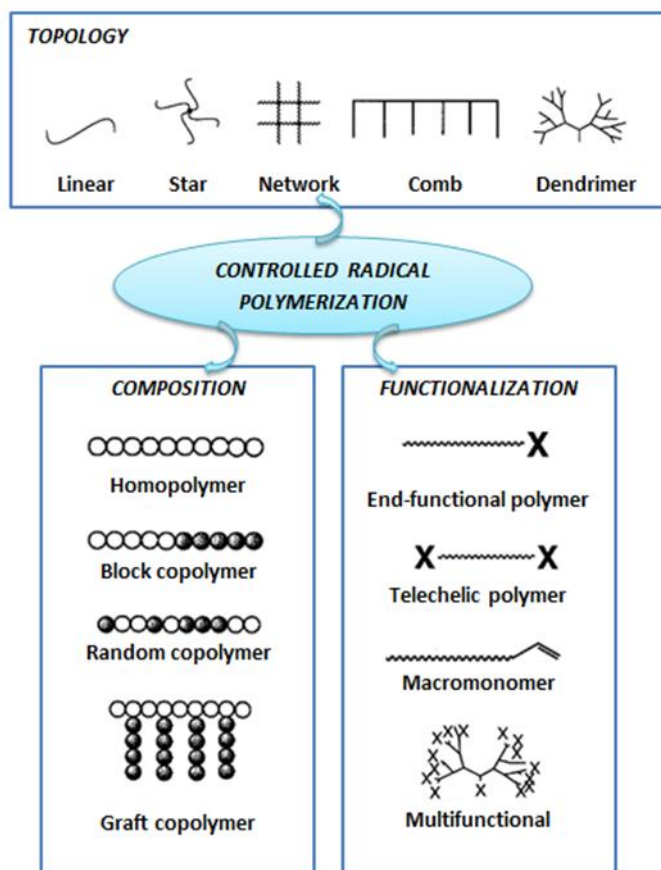


Figure 2.3. Various polymer architectures prepared using CRP [69].

The CRP methods have advantages of obtaining polymeric structures with narrow molecular weights distributions, formation of block copolymers and low sensitive structure against impurities. When the CRP reaction is took place, the main idea is to prevent formation of bimolecular, irreversible termination reaction (in free radical polymerization). Thus, number of growing radical chains must be reduced. Although the reaction becomes slower than free radical polymerization, CRP method provides the good control of molecular weight and very narrow molecular weight distribution [70]. Three main CRP types, namely Atom Transfer Radical Polymerization (ATRP), Nitroxide-Mediated Radical Polymerization (NMP) and Reversible Addition-Fragmentation Chain Transfer Polymerization (RAFT), are explained in details below.

2.2.1. Atom Transfer Radical Polymerization (ATRP)

The atom transfer radical polymerization technique is one particular type of the CRP techniques that have emerged for the treatment of polymers with the desired specific

structures. The ATRP process is robust, versatile and convenient which provides to prepare previously inaccessible well-defined polymeric materials [69, 71, 72].

As shown in Figure 2.4, the ATRP reaction begins with the activation of an alkyl halide (or dormant species), R-X, by the reversible abstraction of the halogen by a low-oxidation-state metal complex shown as $M_t^n\text{-Y/Ligand}$, to reversibly form active radical species, $R\cdot$, which initiates the polymerization. The halogen atom abstraction is reversible, therefore, a dynamic equilibrium is provided between the active species (radicals) and the dormant halogen-capped species. Since, the rate of deactivation, k_{deact} , is very large compared to the rate of activation, k_{act} , the polymer chains are predominantly in the dormant state. The active radical species grow with the rate constant of propagation, k_p , and termination occurs, k_t , similarly to conventional free-radical polymerization. However, the proportion of chains which have been terminated is considerably smaller compared to that of the dormant species. The system, therefore, extremely resembles a living polymerization [73].

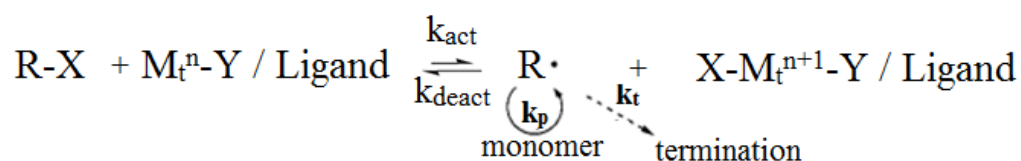


Figure 2.4. Schematic representation of the ATRP process [73].

The long lifetime of the active polymer chains in CRP (and especially in ATRP) lead to synthesis of precise macromolecules with predetermined molecular weights [73]. ATRP is a very versatile technique for the synthesis of a wide range of polymeric structures derived from different types of monomer such as styrenes, [74–76] (meth)acrylates [77], (meth)acrylamides, acrylonitrile, [69, 78] dimethylaminoethyl methacrylate [79] and 4-vinylpyridine except for the polymerization of vinyl acetate and acrylic acids. Recently, interest in this method has increased because of property of realization of reaction of the polymers to be synthesized at room temperature [80]. The main advantage of ATRP is the inexpensive end group composing of simple halogens. However, there are some limitations for ATRP technique. The catalyst must be used for the reaction for ATRP technique. In addition, the catalysts should be removed or recycled at the final

polymerization. Hence, ATRP may be more complicated and may not be the best selection for synthesis of polymeric structure because of the difficulty of obtaining high conversion [81].

2.2.2. Nitroxide-Mediated Polymerization (NMP)

One of the widely used methods of controlled radical polymerization technique to obtain the desired functional and complex polymer structures with well-defined is the nitroxide-mediated polymerization (NMP). This technique was discovered by Dave Solomon in the 1970's and used by many researchers to provide control over the structure of the polymers [82]. The NMP technique is generally defined as the easiest and historically the first applied controlling radical polymerization method [83].

NMP is accomplished by combining monomer (M), radical initiator and nitroxide radical [84]. NMP mechanism is based on a reversible termination mechanism with the propagating polymer radical by the combination of nitroxide, acting as a control agent, to form alkoxyamine active sites as the predominant species. This dormant functionality results in regenerating of the propagating radical and the nitroxide by a simple homolytic cleavage at increasing temperature. When the latter is reasonably selected, equilibrium between successive activation and deactivation reactions is set up (Figure 2.5). This equilibrium offers the advantage of being a purely thermal process without to need to catalyst and bimolecular exchange. The polymerization kinetics is controlled by activation–deactivation parameters (their ratio $k_d/k_c = K$, K is the activation–deactivation equilibrium constant) and the persistent radical effect. The information about these quantities and the factors controlling enables the process of well-defined polymeric structures [85].

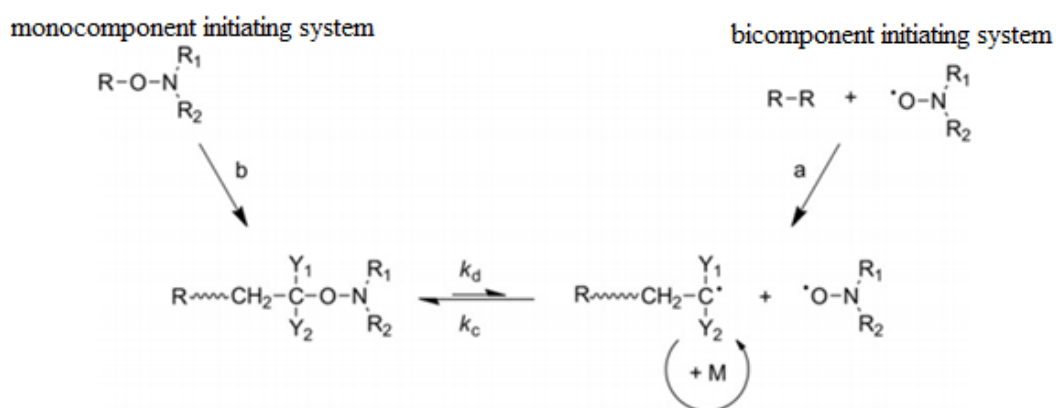


Figure 2.5. The activation-deactivation mechanism in NMP [83].

The first example of NMP was performed with styrene as monomer and TEMPO as the robust nitroxide [86]. NMP provided good control with especially styrene and styrene derivatives [87]. For more challenging polymerization conditions such as high temperature (from 125 to 145 °C) and long time (from 24 to 72 hours), different derivatives of nitroxide are necessary for the success of NMP method, such as 5-, 6-, 7- and 8- membered cyclic nitroxides, acyclic nitroxides, aromatic nitroxides and bis-nitroxides [83]. While this causes some limitations to the use of NMP, the technique still continues to obtain wide variety of polymers and copolymers with controlled structures. Many types of monomer (except for methacrylates) have been polymerized by the NMP method with the use of different nitroxide types [88]. The monomer types that can be successfully and easily polymerized via NMP are styrene and derivatives, vinylpyridines, acrylic esters, acrylic acid, acrylamide, dienes, and acrylates [83]. The development of new nitroxides and alkoxyamines has provided the application of the NMP method to other monomers as well with some exceptions [89].

This method has some main drawbacks such as need of high temperatures and long polymerization times. Although there is great successful for preparation of wide variety of polymer structures and many advantages in simplicity, monomer compatibility and polymer purity [88], another important drawback of NMP is the relatively reduced number of control for monomers due to formation of side reactions and synthetic difficulties associated with nitroxide and restricted works to synthesis alkoxyamine. In particular,

the polymerization of monomers such as vinyl acetate (VAc), vinyl chloride (VC) and N-vinylpyrrolidone (VP) cannot be effectively controlled [83].

Although NMP has been the first CRP technique to be used, ATRP and RAFT have rapidly shown more versatile and better efficiencies in widespread usage areas such as the broader range of controllable monomers, the lower polymerization temperatures, faster polymerization kinetics and many others. Additionally, ATRP and RAFT methods do not require the challenging synthesis of nitroxides and alkoxyamine initiators, as a range of activated alkyl halide initiators for ATRP and thiocarbonyl chain transfer agents (CTAs) for RAFT are commercially ready for polymerization process. The initiators mainly alkyl halides R-X (X = Cl, Br) [67, 90, 91] used for ATRP and the commonly used thiocarbonylthio chain transfer agents such as dithioesters, [53] dithiocarbamates, [53, 92] trithiocarbonates, [93] and xanthates, [94] for RAFT are available to be commercially supplied. According to Nicolas et al. [83], the most significant disadvantage of NMP method is that the polymerization of NVP monomer cannot be successfully controlled. In summary, none of the CRP technique is drawback-free and despite the recent successful studies on NMP, further developments are still necessary.

2.2.3. Reversible Addition-Fragmentation Chain Transfer Polymerization (RAFT)

The reversible addition-fragmentation chain transfer process which was discovered at CSIRO (The Commonwealth Scientific and Industrial Research Organisation) in the 1990s is definitely one of the most usable and effective method of the controlled radical polymerization systems [95]. Even if the theory of atom/group transfer is famous in chemistry, the first reviews about the controlled radical polymerization technique using dithiocarbonyl compounds are discovered in 1998 [96]. Many number of publications conducted over these years have shown that RAFT process is quite successful, versatile and convenient for synthesis of well-defined polymeric architectures [96–100].

Thiocarbonylthio compounds, with a weak carbon-sulphur bond, are used in RAFT process and they provides the key property of living characteristics to radical polymerization [101, 102]. These compounds are able to control the polymerization via a reversible chain transfer process and to grow all the propagating chains proportionally with conversion.

The widely accepted mechanism of chain activation/deactivation for the RAFT is shown in Figure 2.6. The scheme shows the initiation processes, a pre-equilibrium involving the initial RAFT agent, propagation and re-initiation, the addition–fragmentation equilibrium and bimolecular termination reactions. The polymerization mechanism is controlled by a RAFT agent (dithio compound) which is transferred by the reversible addition-fragmentation reaction between dormant and active chains. Propagating macro-radical is added to the RAFT agent in the early stage of the polymerization reaction, and fragmentation of the intermediate macro-radical forms a polymer-RAFT agent compound and a new radical (R^\bullet). Reaction of monomer with R^\bullet creates a new propagating radical (P_m^\bullet). Through rapid equilibrium between the active propagating radicals (P_n^\bullet and P_m^\bullet) and the corresponding dormant species, growth of all chains occurs equally and production of narrow polydispersity polymers are provided. When the polymerization is terminated, the end groups of all chains will retain the thiocarbonylthio functionality end-groups [95].

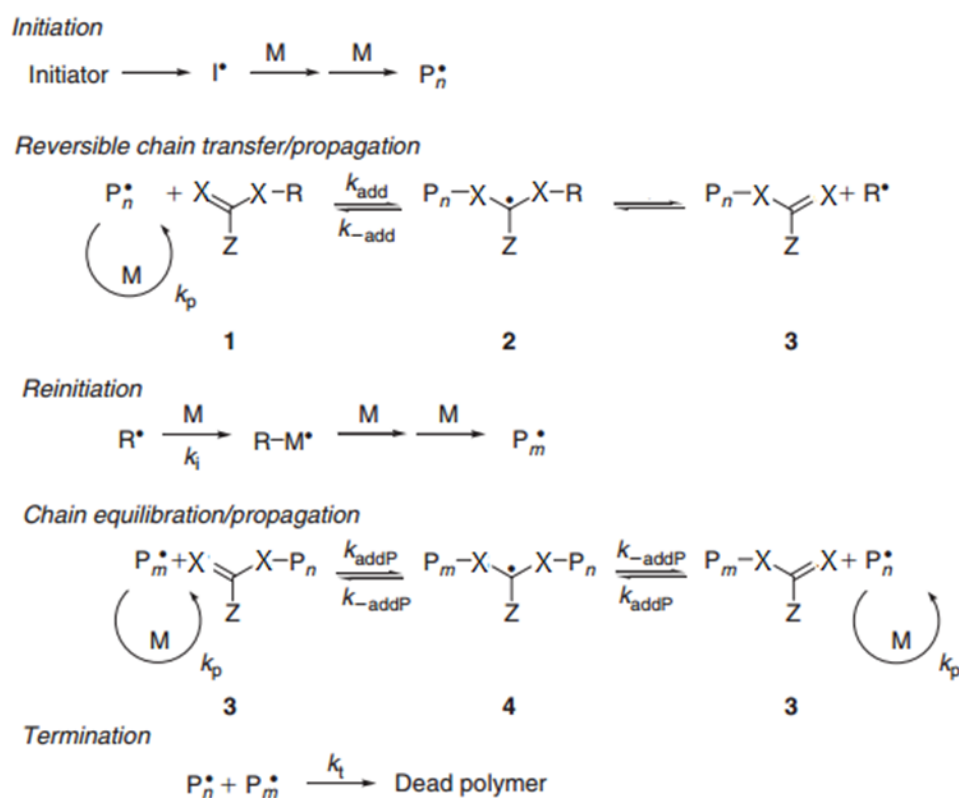


Figure 2.6. Mechanism for reversible addition-fragmentation chain transfer (RAFT) polymerization [95].

The choice of the RAFT agent ($ZC(=S)SR$) for the monomers and reaction conditions is important for the successful RAFT polymerization. The use of appropriate RAFT agent for the monomer provides achievement of well-defined-products and a narrow molecular weight distribution as shown in Figure 2.7.

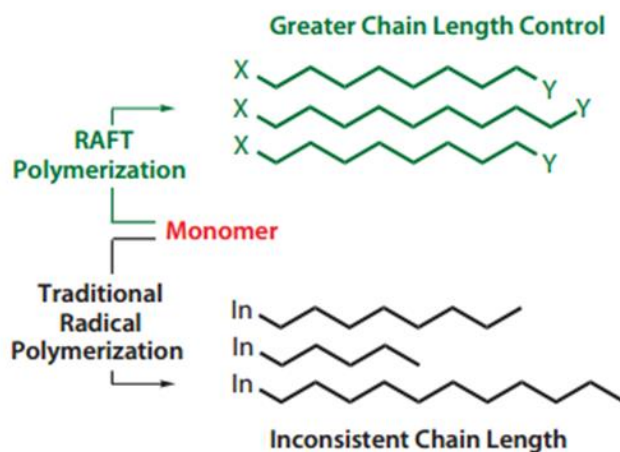


Figure 2.7. Comparison of polymers made with traditional radical polymerization and RAFT process [103].

The effectiveness of the RAFT agents depends on the substituents of X, Z and R groups existing in the common structure of a RAFT agent shown in Figure 2.8. The major effective families of RAFT agents are certain thiocarbonylthio compounds, where Z is a group providing the appropriate reactivity of the RAFT agent, X is sulfur and R is group yielding homolytically leaving free radical that is capable of reinitiating polymerization [96, 104]. There are some different types of thiocarbonylthio RAFT agents including trithiocarbonates ($Z=SR'$), xanthates ($Z=OR'$), dithioesters ($Z=\text{alkyl or aryl}$), and dithiocarbamates ($Z=NR'R''$). The optimal selection of the RAFT agent is depended on the monomer(s), the reaction conditions, and the desired functionality in the product. In order to control the polymerization via RAFT mechanism optimally, choosing an appropriate RAFT agent (R and Z groups) plays an important role [105].

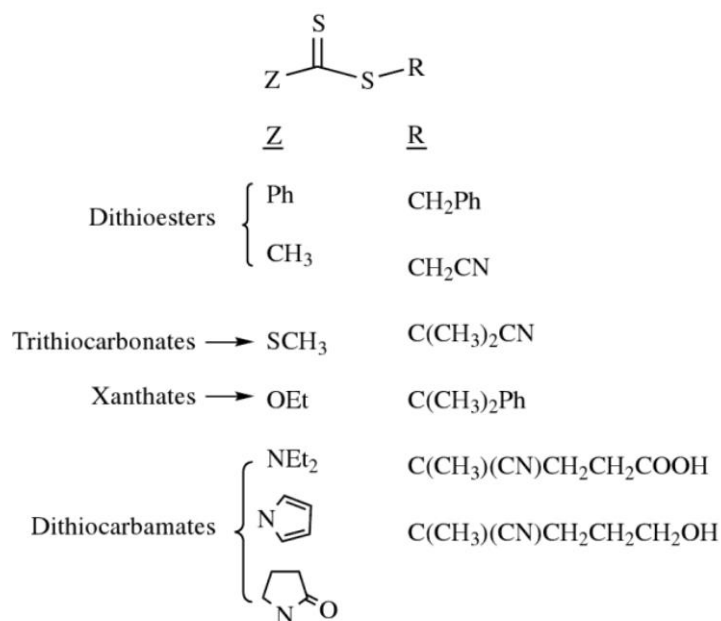


Figure 2.8. General structures of different classes of thiocarbonylthio RAFT agents [105].

The complex polymeric architecture with well-defined homo, gradient, diblock, triblock, graft, comb and star polymers can be prepared by optimal choice of reagents and polymerization conditions for RAFT process [53]. The versatility and effectiveness of this process offers clear advantages over other types of controlled radical polymerization techniques. All chain transfer agents are not compatible with each monomer type and polymerization system. Therefore, determining the optimal conditions reduces side reactions and, hence, improve the living characters of resultant polymers [106]. RAFT polymerization is different from all other CRP techniques, that it can be used with a wide range of monomers, which are difficult to polymerize by other CRP techniques. For example, unprotected (meth)acrylic acids, [107, 108] acrylamides, [107, 109, 110] and vinyl acetate [111] can successfully be synthesized via RAFT polymerization. The RAFT procedure is also regarded as the most tolerant one, and it is compatible with a wide range of polymerization methods such as bulk, solution, emulsion, suspension, etc. Azo-bis-isobutyronitrile (AIBN) or dibenzoyl peroxide initiators used in free radical polymerizations can be also used in the RAFT method. The RAFT process can be carried out in a wide range of temperature from ca. 20 to 150 °C in a wide range of solvents, including water and alcohols under comparatively nondemanding conditions [111]. It has been also used successfully in supercritical carbon dioxide and ionic liquids [99]. As a method having almost the same polymerization conditions with conventional free radical

polymerization, the RAFT process is regarded as more advantageous than NMP and ATRP [112]. theoretical molar mass ($M_{w,theo.}$) is calculated by using equation 7. Since the number of initiator-derived chains are generally small compared to the number of RAFT agent derived chains, the term $2 \cdot f \cdot [I] \cdot \chi$ can be neglected in most cases.

$$Mw_{theo} = \frac{[M] \cdot [Mw_{monomer}]}{[CTA] + 2 \cdot f \cdot [I] \cdot \chi} \cdot \%conv + Mw_{CTA} \quad (Eq. 2.1)$$

Nevertheless, there are some disadvantages of RAFT in comparison to the other CRP systems. If the chain transfer between propagating centers and dormant chain transfer agent (CTA) are dominant, the polymerization can occur very slowly (this case is called as retardation). Furthermore, many RAFT agents (CTA) are toxic, malodorous, colorful and not commercially available or difficult synthesis conditions are necessary [111]. The color and smell of RAFT agents are reflected by the resultant polymer. These drawbacks limit the use of the RAFT method. Although the RAFT process is tolerable for many functionalities and can be used for the polymerization of many monomers, the synthesis of primary or secondary amine end-functional polymers cannot be polymerized by this method, since these functional groups give undesirable side reactions with the RAFT agents [99].

2.3. Surface Functionalization via RAFT Mediated Graft Polymerization and Stabilizing Effect of Surface-attached Grafts

Modifying the surface of various substrates such as polymer films and organic or inorganic particles (e.g. silica, metal nanoparticles, etc) with macromolecular layers or thin films may provide new applications areas and functional units such as recognition sites, catalytic activity, redox-active or bio-active groups, etc. [113]. Among the different substrates available, the surface-functionalized micro- and nano- particles are promising especially due to potential use in catalyst [114]. Among the methods for preparing polymer-coated micro-, nano- particles, grafting of polymer chains is one of the most efficient methods to alter the surface properties by selecting a variety of functional monomers. In this thesis, controlled/living radical polymerization of vinylpyrrolidone (VP) from the surface of the 4,4'-Azobis (4-cyanopentanoic acid) (ACPA) functionalized

silica was carried out. This method provided a micro-particle with an outer layer of covalently attached poly(vinylpyrrolidone), PVP as shown in Figure 2.9. There has been a growing interest in the development of nanometer size particles (nanoparticles) of metals because they offer many applications such as chemical sensors, medicinal science, material science, catalysis and micro-electronics [115]. Metal nanoparticles prepared in suspension generally have an unstable structure which prevents coagulation and precipitation in the solution. However, they can be stabilized by a polymer as represented schematically in Figure 2.9.

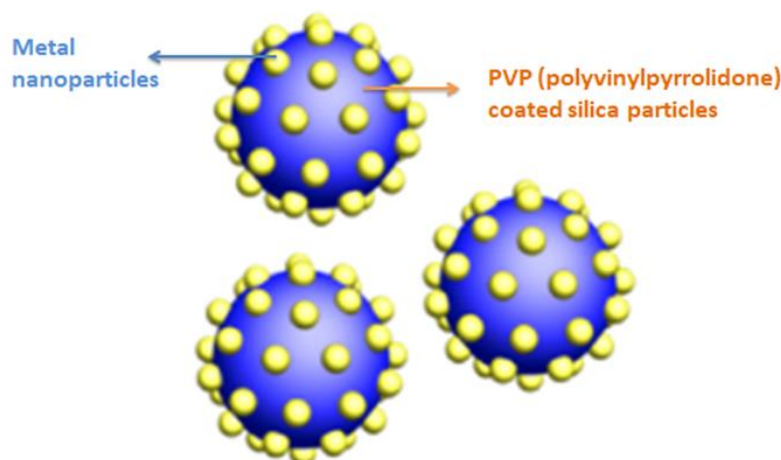


Figure 2.9. Representation of PVP coated silica microparticles with stabilized metal nanoparticles.

2.4. Metal Nanoparticles and Their Stabilization

Recently, the terms nanotechnology, nanoscience, and nanometer size particles have been used widely in application of scientific and engineering fields. It was found that metal nanoparticles are very applicable and useful in catalytic fields. There are many different optical, chemical and physical properties for metal nanoparticles than those of bulk metals. The major problem in working with nanoparticles is their undesirable agglomeration to generate larger particles. In order to prevent formation of agglomerates, protecting polymers [115], ligand exchange materials, [93,116] and surfactants [117, 118] are used. They provide stability during the formation of nanoparticles and therefore suppress the aggregation [119].

Metal nanoparticles cannot be thermodynamically stable due to their large surface energy and chemical activity, therefore they tend to oxidize and agglomerate easily when exposed to moisture or air [120]. This situation negatively affects the properties of metal nanoparticles and limits their use in many applications. The metal nanoparticles can be stabilized by embedding them in solid host materials. The host material to be used should be selected according to the area of use of metal nanoparticles. Another approach to stabilize the metal nanoparticles is to interact them with a support material in solution, such as solvated polymers. The stability of metal nanoparticles is generally based on electrostatic or steric interactions [121].

The role of polymeric supports (surfactants or ligands) attached on metal nanoparticles in their protection is very significant since these polymers stabilize metallic NPs through steric hindrances (Figure 2.10). The functional groups of polymers such as amines, carboxylic acids, tiols, silanes, phosphines, etc. provide the anchoring of the molecule at the cluster surface [122]. When nanoparticles are prepared by irradiation, the stabilizers should not reduce the ions before irradiation. Some stabilizers used in the synthesis of nanoparticles such as poly(vinyl pyrrolidone) (PVP), poly(vinyl alcohol) (PVA), poly(acrylamide) (PAM), sodium poly(vinyl sulfate) (PVS), poly(ethylene imine) (PEI), sodium dodecyl sulfate (SDS), and poly(N-methyl acrylamide) (PNMAM) fulfill the criteria for stabilizations [123]. However, the most commonly used polymer stabilizers are PVA and PVP though others have also reported [124]. PVP is generally chosen for radiolytic reduction processes due to excellent properties such as large protective value and high solubility in water [4]. In this M.S. thesis, formation of the palladium nanoparticles was examined by reduction of palladium (II) in the presence of protective PVP.

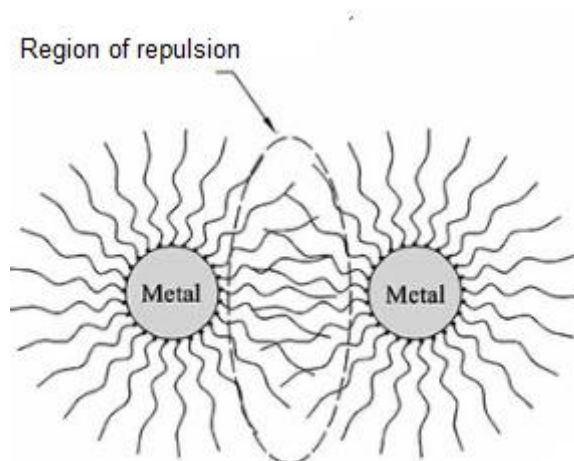


Figure 2.10. Steric stabilization of metallic nanoclusters [124].

2.5. Preparation of Metal Nanoparticles by Ionizing Radiation

The discovery of X-rays by the German physicist Wilhelm Conrad Röntgen in 1895 [125] and the discovery of uranium degradation by Becquerel in 1896 [126] have marked a turning point in the scientific world. X-rays have been only used for many years to reduce silver ions to silver atoms and then to fog the photographic plates with the silver metal clusters formed by the combination of silver atoms [127].

It has been known since the beginning of the researches in the field of nanotechnology that nanomaterials can be prepared by using ionizing radiation (gamma, X-rays and accelerated electrons). Ionizing radiation plays an important role in the preparation of nano-structured materials, catalysts, biosensors, nano-gels, opto-electronics, biological labelling, nano-electronic chips, and magnetic separators [128–130]. In addition to these application areas, the advantages of ionizing radiation are also used in the preparation of metal nanoparticles. Reduction of metal ions by ionizing radiation and the preparation of metal nanoparticles have many advantages over the preparation of metal nanoparticles using other methods of reduction (chemical, thermal, photochemical, electrochemical) [131].

Advantages of using ionizing radiation in the synthesis of metal nanoparticles compared to other methods are given as follows. These are;

- High reduction potential of the reducing species generated by irradiation,
- The production of nanoparticles from metal ions including noble metal ions,

- The fast kinetics of metal ion reduction at ambient temperature without excessive chemical reducing agent
- Control size and size distribution of the obtained metal nanoparticles [132].

There are two general classes of ionizing radiation or high energy radiation: directly ionizing radiation and indirectly ionizing radiation. High-speed electrons with charged beams directly ionize the types of α (alpha) and β (beta) particles. High-energy electromagnetic waves (gamma, X-rays) and high-speed neutral particles deliver their energies into charged particles where they do not directly ionize matter [133]. The types of ionizing radiation are seen in the high frequency (f), low wavelength (λ) region on the right side of the electromagnetic spectrum in Figure 2.11 [134].

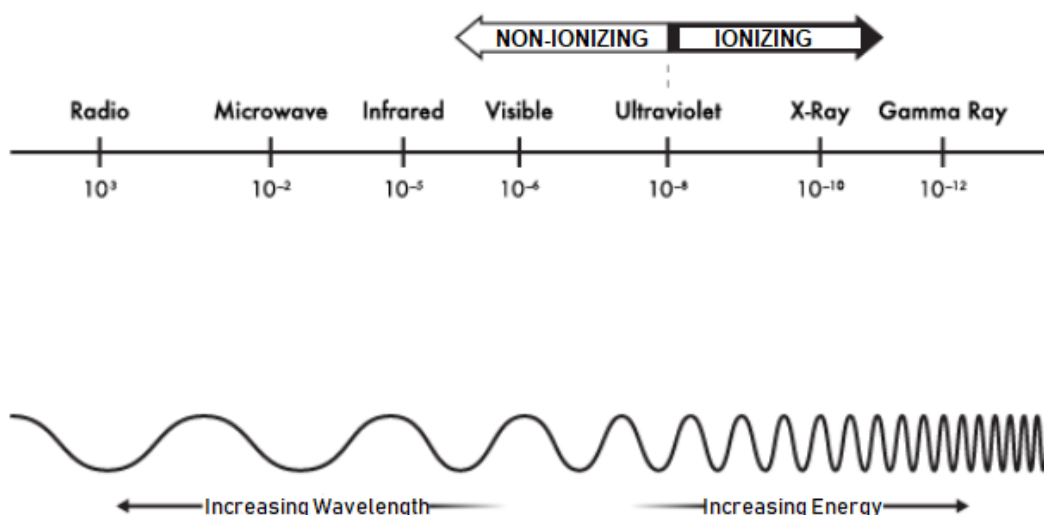
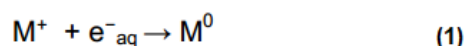


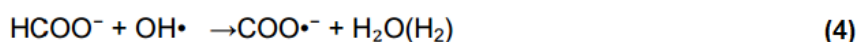
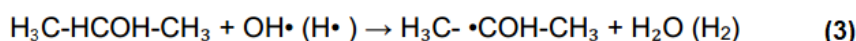
Figure 2.10. The electromagnetic spectrum illustrating the range of frequencies of all radiation.

The synthesis of metallic nanoparticle is generally carried out by chemical reduction of metal precursor salts in aqueous medium. The radiochemical method by gamma-irradiation is used to form hydrated electrons by means of water radiolysis, which ensures distribution homogeneously in the medium, these species can easily react with solvated metal ions reducing their oxidation state [135]. This technique provides homogeneous reduction and balance between the nucleation rate and the particle growth and further yields controlled size, shape and structure. In radiolytic reduction process oxidizing and

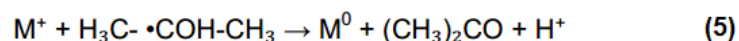
reducing species are formed such as “hydrated electrons” (e_{aq}^-) and “hydrogen atoms” ($H\bullet$), where the solvated electrons and $H\bullet$ possess reductive potential $E^0 (H_2O/e_{aq}^-) = -2.87$ V and $E^0 (H^+/H\bullet) = -2.3$ V (showing the below Eqs. 1 and 2), while the $OH\bullet$ has the strong oxidative potential $E^0 (OH\bullet/H_2O) = +2.8$ V, which would provide a high oxidation state to the metal ions or atoms [136].



The presence of this species causes the metal atoms formed by reducing species to be re-oxidized with $OH\bullet$ radicals. In order to avoid oxidation reactions, additives such as secondary alcohols or formate anions ($HCOO^-$) having the scavenging properties for $OH\bullet$ radicals are introduced to the reaction medium. Hydrogen radicals which have reductive properties are also removed by these scavengers.



The radicals $H_3C-\bullet COH-CH_3$ (3) and $COO\bullet^-$ (4) formed as a result of these reactions are powerful reducing agents. [$E^0 (CH_3)_2CO / H_3C-\bullet COH-CH_3) = -1.8$ V and $E^0 (CO_2/COO\bullet^-) = -1.9$ V] as shown in following equations [137].



The binding energy between two metal atoms is much stronger than the bond energies between the metal atom-solvent and the metal atom-ligand. Therefore, the metal atoms come together to form the nanoclusters [136]. Under irradiation, the metal atoms formed as a result of the reduction are homogeneously dispersed throughout the solution. The radiation technique has approved to be a more environmentally friendly and cost-effective

process for generation of a large quantity of shape and size controllable metal nanoparticles [138, 7, 139].

2.5.1. The Effect of Radiation Dose Rate and Absorbed Dose

In the reduction of ionic structures by the effect of ionizing radiation and the reduction of ionic structures, the dose rate of the radiation source with the absorbed dose affects the number and quality of the reduced species. Dose refers the energy absorbed per unit mass and the dose rate refers to the number of photons emitted by the radioactive source per unit time. The absorbed dose affects the amount of the species formed and the dose rate affects the rate of formation of the active species [140].

The irradiation dose rate is an important factor affecting the quantity, shape and size of the nanoparticles. Decreasing the irradiation dose rate slows the rate of formation of reducing agents. In this case, large metal nanoclusters are formed with a sufficient number of metallic cores [141]. In the irradiation at high dose rate, the reducing agents quickly reduce the metal ions and cause the formation of many smaller clusters. In this case, a large number of clusters formed cannot grow sufficiently, since these clusters do not interact with metal ions a large number of small metal nanoparticles are formed (Figure 2.12) [138].

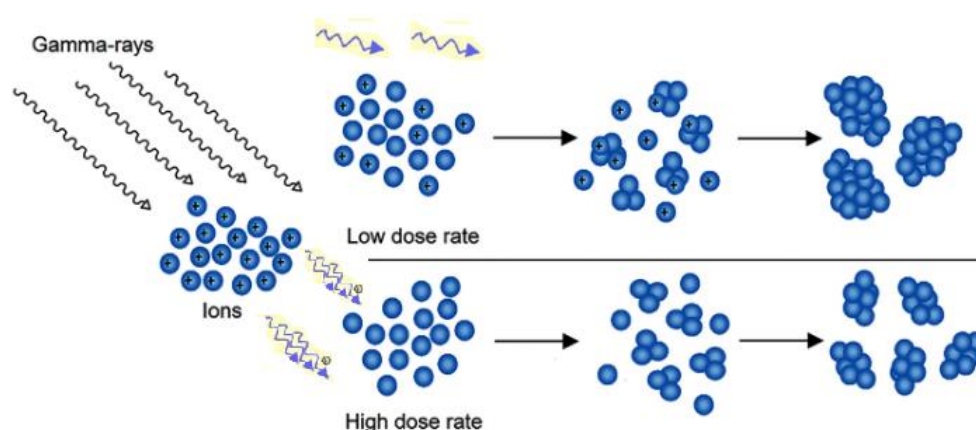


Figure 2.11. The effect of dose rate on the size of nanoclusters generated [4].

3. EXPERIMENTAL

3.1. Materials

3-Aminopropyl-functionalized silica (~1 mmol/g NH₂ loading, 40 μm average particle size, 550 m²/g surface area, 60 Å pore size), 4,4'-Azobis (4-cyanopentanoic acid) (ACPA), N,N' dicyclohexyl carbodiimide (DCC), palladium (II) acetate (Pd(OAc)₂), 4-nitrophenol (4-NP), 4-aminophenol (4-AP), sodium borohydride (NaBH₄), N-vinylpyrrolidone (VP), ethanol (EtOH), potassium ethyl xanthogenate (PAX) and methyl-2-bromopropionate (MB) were purchased from Sigma-Aldrich. A xanthate (dithiocarbonate) type RAFT agent, namely O-ethyl-S-(1-methoxycarbonyl) ethyl dithiocarbonate (RA1), was selected as it is suitable for less activated monomers, such as VP, and synthesized using PAX and MB. [142]

3.2. Attenuated Total Reflectance Fourier Transform Infra-Red (ATR-FTIR) Spectroscopy

FTIR spectra were recorded in attenuated total reflection (ATR) mode by Perkin Elmer Spectrum One model spectrometer. Spectra were obtained by 32 scans with a 4 cm⁻¹ resolution.

3.3. X-Ray Photoelectron Spectroscopy (XPS)

X-ray photoelectron experiments were carried out using mono-chromatized Al K α X-ray source of Thermo spectrometer using an X-ray spot size of 400 μm. 30 eV and 200 eV pass energies were applied during the survey and region scans, respectively. Binding energies (BEs) were referenced to the C1s peak at 285 eV and surface elemental compositions were determined by varying the energy between 0-1000 eV.

3.4. UV-Vis Spectroscopy

The absorbance of target molecules was measured by Varian Cary100 model UV-Vis spectrophotometer between 200-600 nm wavelength at room temperature.

3.5. Dynamic Light-Scattering (DLS)

The average hydrodynamic diameter of free Pd NPs or relative products in irradiated solutions were measured using Zetasizer Nano ZS (Malvern Instruments Ltd., UK) equipped with a 4 mW He-Ne laser (633 nm wavelength). All the experiments were carried out at constant temperature, 25 °C, with at least three successive measurements.

3.6. Atomic Force Microscopy (AFM)

Changes on the surface morphology were investigated using MultiMode V AFM with Nanoscope 9.1 controller (Bruker) in tapping mode in air.

3.7. Scanning Electron Microscopy (SEM) Imaging and Energy Dispersive X-Ray (EDX) Mapping

FEI Quanta 200FEG microscope was used to take the SEM images of samples at different magnifications. The samples were covered with Au/Pt (10 nm) before imaging. For the attainment of elemental mappings, Supra 35VP Leo EDX instrument was used.

3.8. Transmission Electron Microscopy (TEM)

FEI Tecnai G2 F30 transmission electron microscope (TEM) operated at 100 keV was used for imaging.

3.9. Size Exclusion Chromatography (SEC) Analysis

The molecular weight distributions of free, i.e. non-grafted, PVP chains in solution were analysed by SEC. Molecular weight data for the PVP samples were obtained using an Agilent 1100 gel permeation chromatograph with PL aquagel-OH column standards in water (0.1M NaNO₃) as a mobile phase at 25 °C. Poly(ethylene glycol) (PEG) and poly(ethylene oxide) (PEO) were used as standarts. The monomer conversion was determined by gravimetric measurement. GPC results were calculated on the basis of calibration with narrowly distributed PEG and PEO standarts without using Mark-Houwink constants as they are not available. Therefore, the values *M_n* and PD reported are not true values but instead correspond to PEG and PEO equivalents. As PEG and

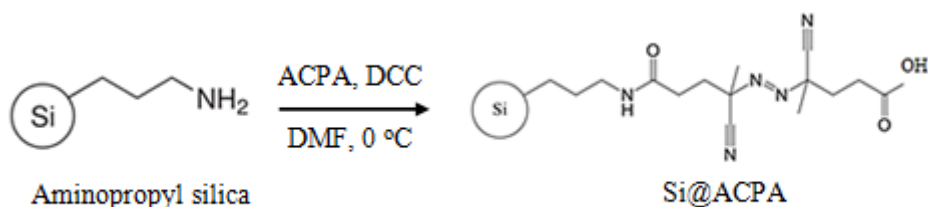
PEO are commonly regarded as suitable standards for PVP, we believe that the results are reliable, especially for comparison purposes.

3.10. Thermogravimetric Analysis (TGA)

TGA was performed to study the changes in thermal stability and decomposition of the substrate and grafted materials. Thermal decomposition properties of samples were recorded using a Perkin Elmer thermogravimetric analyzer (Pyris 1 TGA). Analyses were conducted over the temperature range from 25 to 700 °C with a programmed temperature increment of 10 °C min⁻¹ under N₂ atmosphere.

3.11. Synthesis of 4,4'-Azobis(4-cyanopentanoic acid) (ACPA) Functionalized Silica (Si@ACPA)

1 g ACPA and 0.8 g DCC was dissolved in 50 mL DMF. This solution was added dropwise to a suspension of 2.0 g NH₂-functionalized silica in 20 mL DMF during vigorous stirring. The reaction mixture was stirred at dark for 48 hours at 0 °C and Si@ACPA was filtered through Whatman No. 1 filter paper and dried under vacuum at room temperature [45]. Si@ACPA macro-initiator (Scheme 3.1) was kept in dark below 0 °C.



Scheme 3.1. Schematic Representation of the Synthesis of the Azo Initiator Modified Silica microparticles (Si@ACPA).

3.12. Synthesis of Poly(vinylpyrrolidone) (PVP) Grafted Silica Micro-particles (Si@PVP)

PVP chains with different target lengths were grafted from silica core using Si@ACPA as the macroinitiator via RAFT-mediated graft polymerization as summarized in Table 4.1. From the sample code in Table 4.1, the number used after PVP denotes the target

molecular weight of PVP at complete monomer conversion while the second is for the polymerization time. In a typical grafting, VP (2.81 g, 25.3 mmol) and desired amount of RA1 (e.g. 0.14 mmol) was dissolved in 10 mL water and 0.10 g of Si@ACPA macroinitiator was added to reaction medium. 1.67 mg (5.96×10^{-3} mmol) ACPA was added to mixture along with the initiating sites that exist on the surface of Si@ACPA as addition of free ACPA to the solution provides better control of the growth of surface adherent chains [19]. The grafting solution in a round bottom reaction vessel was sealed, purged with nitrogen gas for 15 min and placed in a shaking (100 rpm), thermostated bath at 65 °C for different time intervals. At the ends of the predetermined polymerization periods, PVP grafted silica samples (Si@PVP) were filtered, washed several times with deionized water to remove free homopolymer and then dried under vacuum at 50 °C for 24 h.

3.13. Formation of Palladium Nanoparticles Stabilized by PVP (Si@PVP-PdNP):

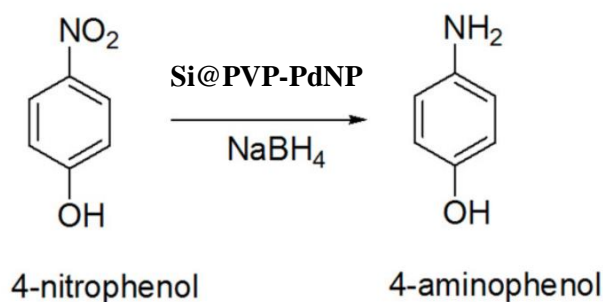
Prior to radiolytic reduction of Pd(II) ions to Pd metal NPs, predetermined amounts of Si@PVP with different graft chain lengths (Si@PVP20, Si@PVP33 or Si@PVP50) were subjected to 15 mL of 0.45 M Pd(OAc)₂ precursor solution in sealed tubes and shaken at 100 rpm at room temperature for 24 h to ensure maximum Pd(II) ion absorption. The amount of Si@PVP in the mixture was set to Pd:VP mol ratio of 1:1 or 1:10 using the PVP grafting degrees calculated by TGA analysis (see Table 4.1). For example, the mass of Si@PVP50-10h sample with a DG of 19.9 % (w/w) was either 3.77 mg (1:1) or 37.7 mg (1:10). The mixtures were then purged with N₂ gas for 20 min and irradiated at room temperature using a Co-60 gamma cell at Sarayköy, TAEK. The total absorbed dose was 10 kGy for all samples. Three different solvents, namely water, ethanol or ethanol:water (40:60, v/v), were used for the preparation of the mixtures in order to observe the effect of reduction medium on the formation of Pd NPs. After irradiation, Si@PVP-PdNP samples were collected by filtration and washed with deionized water several times and finally stored in acetone. The filtrate was kept for DLS analysis.

3.14. Catalytic Activity Measurements

The reduction of 4-NP to 4-AP (Scheme 3.2) by NaBH₄ was chosen as a model reaction for investigating the catalytic performance of Si@PVP-PdNP samples. Typically,

10 mL of 7.82×10^{-3} M NaBH_4 solution was added to 10 ml 4-NP aqueous solution with an initial concentration of 7.82×10^{-6} M under stirring (100 rpm). Subsequently, 5.0 mg of Si@PVP-PdNP catalyst sample was added to the above solution at constant temperature and the consumption of 4-NP was monitored periodically by the decrease of its absorption peak located at 400 nm via UV-Vis Spectroscopy. The use of an excess of NaBH_4 ensures that its concentration remains essentially constant during the reaction, which permits the assumption of pseudo-first-order kinetics with respect to the nitro compound. Once the reaction was completed, the Si@PVP-PdNP catalyst was removed from the solution by filtration (Whatman filter paper no. 1), thoroughly rinsed with deionized water and then recycled without drying for three times in the same procedure.

After the first run of reaction, the catalyst was isolated by filtration through Whatman No. 1 filter paper and dried under vacuum at room temperature, then bottled in acetone. The bottled samples of Si@PVP-PdNP were then isolated, dried, weighed and reused in the reduction of 4-NP to 4-AP after 1, 2, 3 and 5 week. The reusability of the catalyst system was evaluated by measuring the amount of 4-NP reduced per mass of Si@PVP-PdNP from the decrease in absorbance at 400 nm once the reaction was completed.



Scheme 3.2. Schematic Representation of Reduction of *p*-Nitrophenol to *p*-Aminophenol.

4. RESULT AND DISCUSSION

The covalent attachment of polymers on a surface can be obtained through either a ‘grafting to’ or ‘grafting from’ technique. In the ‘grafting from’ approach, uniform polymer brush layers of a high grafting density can be obtained [143]. The free, i.e. nongrafted, polymers formed in solution are good indicators of grafted chains in a ‘grafting from’ approach [23]. Therefore, analyzing the properties of free polymers gives important information about the grafted ones. Table 4.1 summarizes some experimental conditions applied during the synthesis of PVP grafted silica samples. Molecular weights and polydispersities of free, i.e. non-grafted PVP chains, attained by SEC and grafting degrees (mass of grafted PVP to mass of silica substrate) calculated based on TGA were also presented in the same table. The controlled fashion of grafting is showed in Table 4.1 and corresponding figures (Figure 4.1 a-c), where narrow and unimodal chromatograms and linear evolution of the number-average molecular weight, M_n , with conversion (which is expected for a controlled/living polymerization), is depicted. Furthermore, the PD values remain in the range of 1.35–1.65. The agreement with the theoretical number-average molecular weight, $M_{n,thr.}$, is also good for all RAFT mediated graft polymerizations. The theoretical number-average molecular weight can be calculated using the following equation.

$$M_{n,thr} = \frac{[Monomer]}{[RAFT]} \times [Mw, monomer] \times Conv (\%) + Mw, Raft \quad (Eq. 4.1)$$

In addition to the RAFT mediated grafting of PVP, conventional graft polymerizations were also achieved for two samples (denoted as control in Table 4.1) and results clearly demonstrate the uncontrolled fashion of the polymerization in the absence of chain transfer agent, RA1. The sample with code ‘Si@NH₂-8h’ is free of surface-immobilized ACPA initiator. As seen from the table, no grafting takes place for this sample, suggesting that the attachment of PVP chains to the surface is by chemical bonds rather than by

physical means. Also, this sample shows that cleaning procedure applied to remove the physically attached polymer chains from the silica surface was efficient.

Table 4.1. Reversible addition fragmentation chain transfer (RAFT) mediated grafting of N-vinylpyrrolidone (VP) from silica surface in water at 65 °C with RA1 as RAFT agent, [VP] = 2.53 M.

| Sample Code ^a | [VP]/ [RA1] | RA1 ^b (mmol) | Conv. ^c (%) | $M_{n,thr.}$ ^d (g/mol) | $M_{n,exp.}$ ^e (g/mol) | PD ^e | GD ^f (%, w/w) | Time (h) |
|-------------------------------------|----------------|----------------------------|---------------------------|--------------------------------------|--------------------------------------|-----------------|-----------------------------|-------------|
| Si@PVP20-8h | 180 | 0.140 | 33.1 | 6830 | 11900 | 1.50 | 1.9 | 8 |
| Si@PVP33-8h | 300 | 0.084 | 49.7 | 16770 | 25600 | 1.45 | 8.9 | 8 |
| Si@PVP50-8h | 452 | 0.056 | 57.0 | 28830 | 39000 | 1.41 | 17.8 | 8 |
| Si@PVP84-8h | 760 | 0.033 | 81.1 | 68690 | 78500 | 1.60 | 19.5 | 8 |
| Si@PVP50-2h | 452 | 0.056 | 21.1 | 10800 | 15100 | 1.65 | 13.0 | 2 |
| Si@PVP50-5h | 452 | 0.056 | 30.3 | 15420 | 21100 | 1.51 | 15.4 | 5 |
| Si@PVP50-10h | 452 | 0.056 | 70.7 | 35710 | 47100 | 1.35 | 19.9 | 10 |
| Control ^g | - | - | - | - | 112100 | 2.49 | 17.6 | 2 |
| Control ^g | - | - | - | - | 131000 | 2.71 | 24.2 | 8 |
| Si@NH ₂ -8h ^h | 452 | 0.056 | 33.7 | 17130 | 27100 | 1.42 | 0 | 8 |

^aThe number used after PVP indicates the target molecular weight of PVP at complete monomer conversion (i.e. 20.200, 33.540, 50.425, or 84.640 g/mol) while the second one denotes the polymerization time. ^bO-ethyl-S-(1-methoxycarbonyl) ethyl dithiocarbonate (208.3 g/mol). ^cMonomer conversion was determined gravimetrically by evaporating the filtrates of polymerization solution, ^dTheoretical number-average molecular weight, $M_{n,thr.}$, was calculated from the monomer conversion using Eq. 4.1 based on Eq. 2.1. ^eNumber average molecular weight, $M_{n,exp.}$, and polydispersity, PD, determined via size-exclusion chromatography, SEC, using water (0.1 M NaNO₃) as eluent with PEG and PEO standards. ^fGrafting degree (mass of grafted PVP to mass of silica substrate) was calculated from the TGA results, ^gConventional grafting results of VP (25.3 mmol) in water at 65 °C. ^hInitiator-free silica surface (Si@NH₂) was employed in grafting.

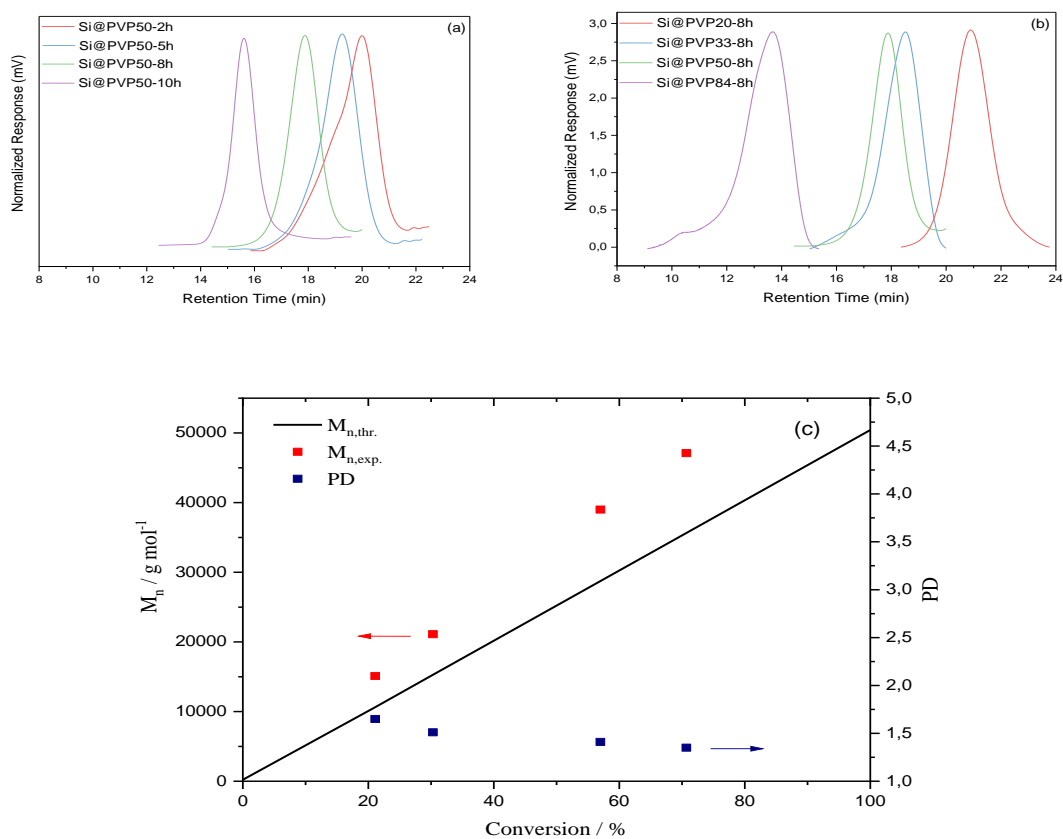


Figure 4.1. GPC chromatograms as a function of (a) polymerization time, (b) VP/RA1 molar ratio. (c) Experimental and theoretical number-average of molecular weights as a function of monomer conversion and PD values obtained by using VP/RA1: 452 molar ratio.

Thermogravimetric analysis (TGA) was used because it is a very practical and reliable method for determining the grafting degree (GD) of the Si@PVP samples. As seen in Figure 4.2a, the thermal degradation process of PVP homopolymer in N_2 atmosphere shows one main weight loss starting at around 380 °C and continues up to 520 °C. The maximum degradation rate is reached at 472 °C (derivative thermogravimetry curve not presented here) and the residue at 700 °C is 2.5 %. The degradation profile of the grafted samples contains multiple steps corresponding to degradations of 3-aminopropyl, ACPA and PVP functionalities (see Figure 4.2b and 4.2c).

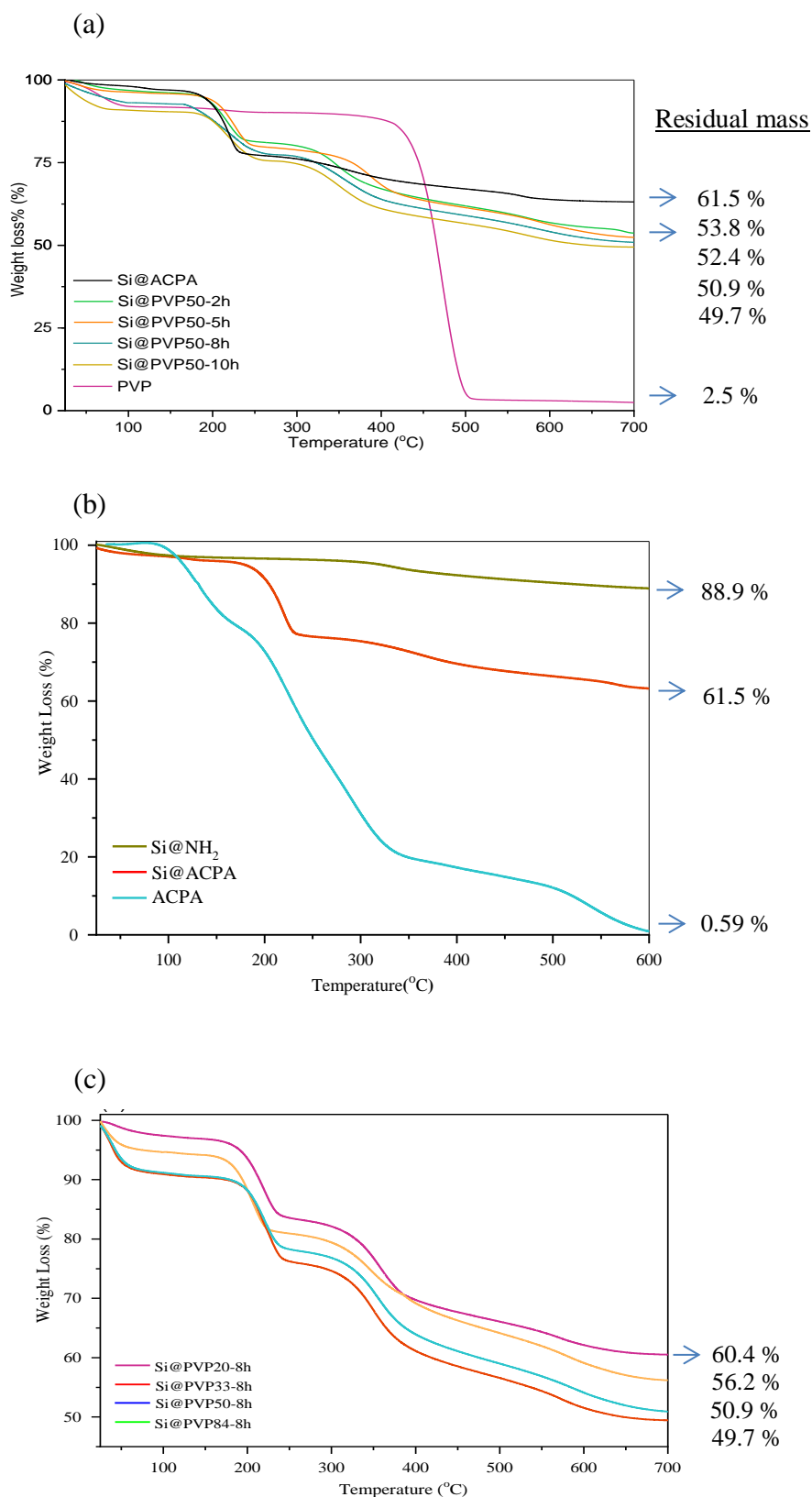


Figure 4.2. TGA thermograms of (a) initiator-immobilized silica (Si@ACPA), PVP and PVP grafted silica (Si@PVP) samples with different polymerization time, (b) Si@NH₂, ACPA and Si@ACPA, (c) Si@PVP samples with different target molecular weights. Target chain length was derivatized by changing the [VP]/[RA1] molar ratio.

Using the residual masses in Figure 4.2, the grafting degree (GD) of each sample was calculated using the following method shown for the sample coded “Si@PVP50-2h”. The grafting degree (GD) for each sample code was calculated by using the residual amount of TGA curves and the GD values was recorded in the Table 4.1.

Grafting density ;

for **Si@PVP50-2h**;

Si-ACPA : 61.5 %
PVP : 2.5 %
Si@PVP50-2h: 53.8 %

}

A % Si@ACPA
100-A % PVP

$$A \times 0.615 + (100 - A) \times (0.025) = 100 \times (0.538)$$

A = 87 % Si
13 % grafted PVP

The amount of residue decreases with polymerization time, indicating a higher PVP content in Si@PVP samples. As polymerization progresses, more initiating species, i.e. radicals, form on silica surface as a result of homolytic cleavage of ACPA, subsequently yielding more grafted chains. In addition, longer chains are attained at higher conversion, and hence at longer polymerization times in Table 4.1 as the M_n is a linear function of monomer conversion in RAFT polymerization. Figure 4.2c shows that increasing VP/RA1 molar ratio results in higher GD at the same polymerization time. This clearly indicates the formation of longer PVP grafts on the silica surface, as an expected outcome of the RAFT mechanism.

In order to structurally characterize the grafted PVP shell we performed FTIR analysis (Figure 4.3). Grafting of PVP to silica significantly led to appearance of C=O peak at around 1650 cm^{-1} [144] in addition to already existing carbonyl peak of immobilized ACPA functionalities (see Figure 4.4). The intensity of this peak increases with polymerization time, indicating an increase in GD of PVP in agreement with the results in Table 4.1. C-H stretching peak and C–H bending vibration of PVP, appearing at 2930 cm^{-1} and 1436 cm^{-1} , respectively, become more distinct by increasing GD of PVP [145]. C–N stretching vibration at 1286 cm^{-1} is overlapped by the strong absorption peaks of Si@NH₂

(Figure 4.4). The absorption band around 3500 cm^{-1} can be ascribed to water absorbed by PVP and it is also noticeable in TGA with mass loss before $100\text{ }^{\circ}\text{C}$.

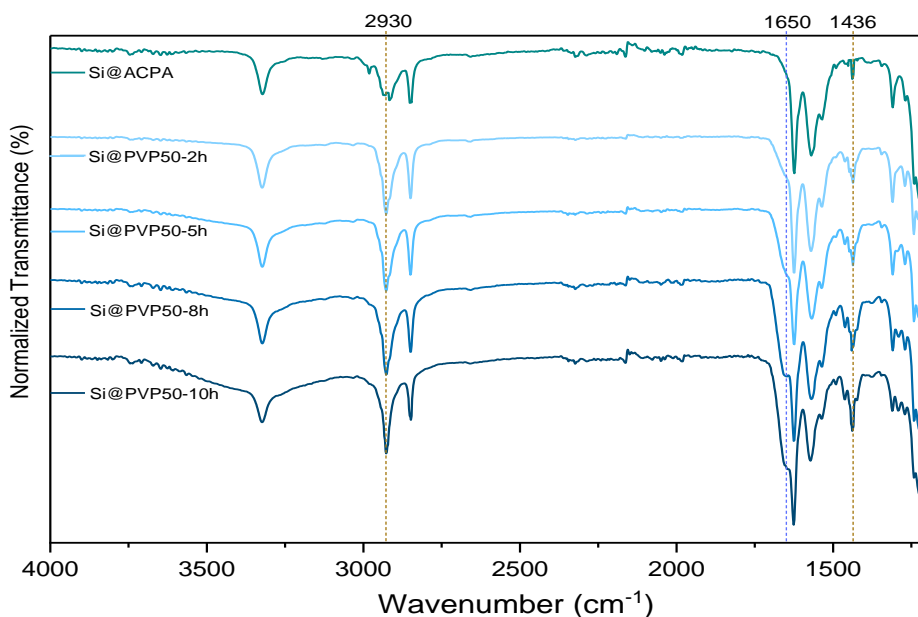


Figure 4.3. FTIR spectra of initiator-immobilized silica (Si@ACPA) and PVP grafted silica (Si@PVP) samples.

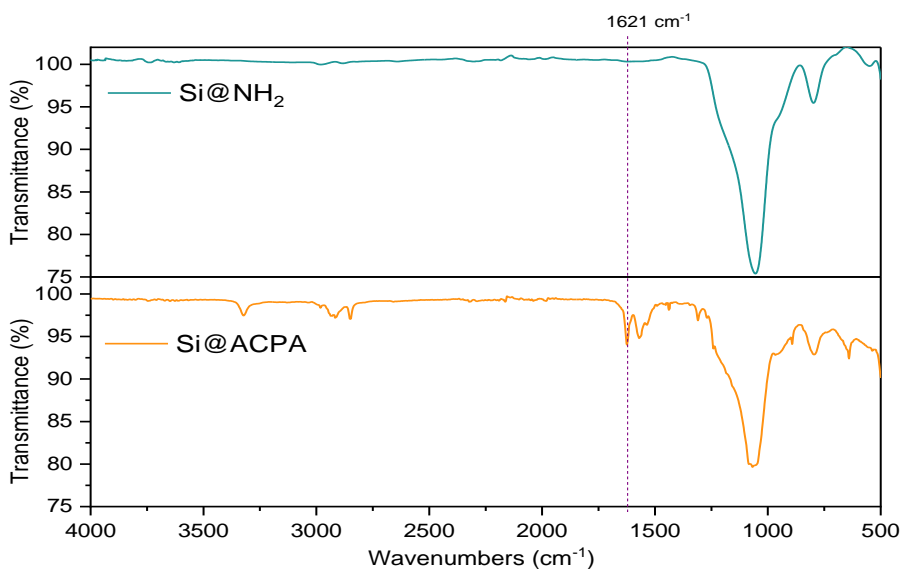


Figure 4.4. Comparison of FTIR spectrum of Si@NH₂ and Si@ACPA. The carbonyl (C=O) peak of ACPA appears at 1621 cm^{-1} .

In order to investigate the morphological behavior, we have performed SEM analysis as presented in Figure 4.5. As can be seen in this figure, PVP grafted surface looks free from any spurious matter such as aggregated PVP domains. This indicates that a homogeneous surface coverage took place during the grafting of PVP from silica surface. SEM-EDX mappings presented in Figure 4.6, illustrate the distribution of Si (blue) and N (red) elements across the image. Obviously, the nitrogen content increases on the silica surface following the grafting which proves the attachment of PVP chains. Homogeneous distribution of this element through the surface indicates a uniform surface coverage.

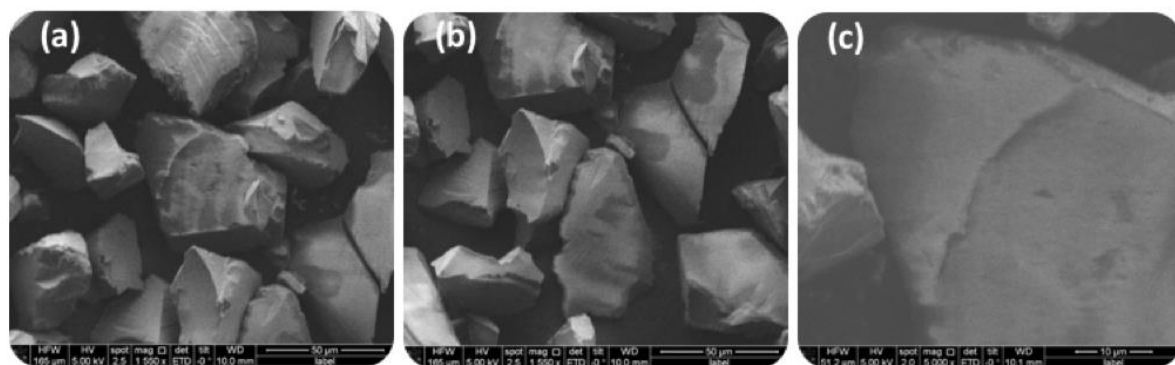


Figure 4.5. SEM images of (a) Si@NH₂, (b) Si@ACPA and (c) Si@PVP50-8h

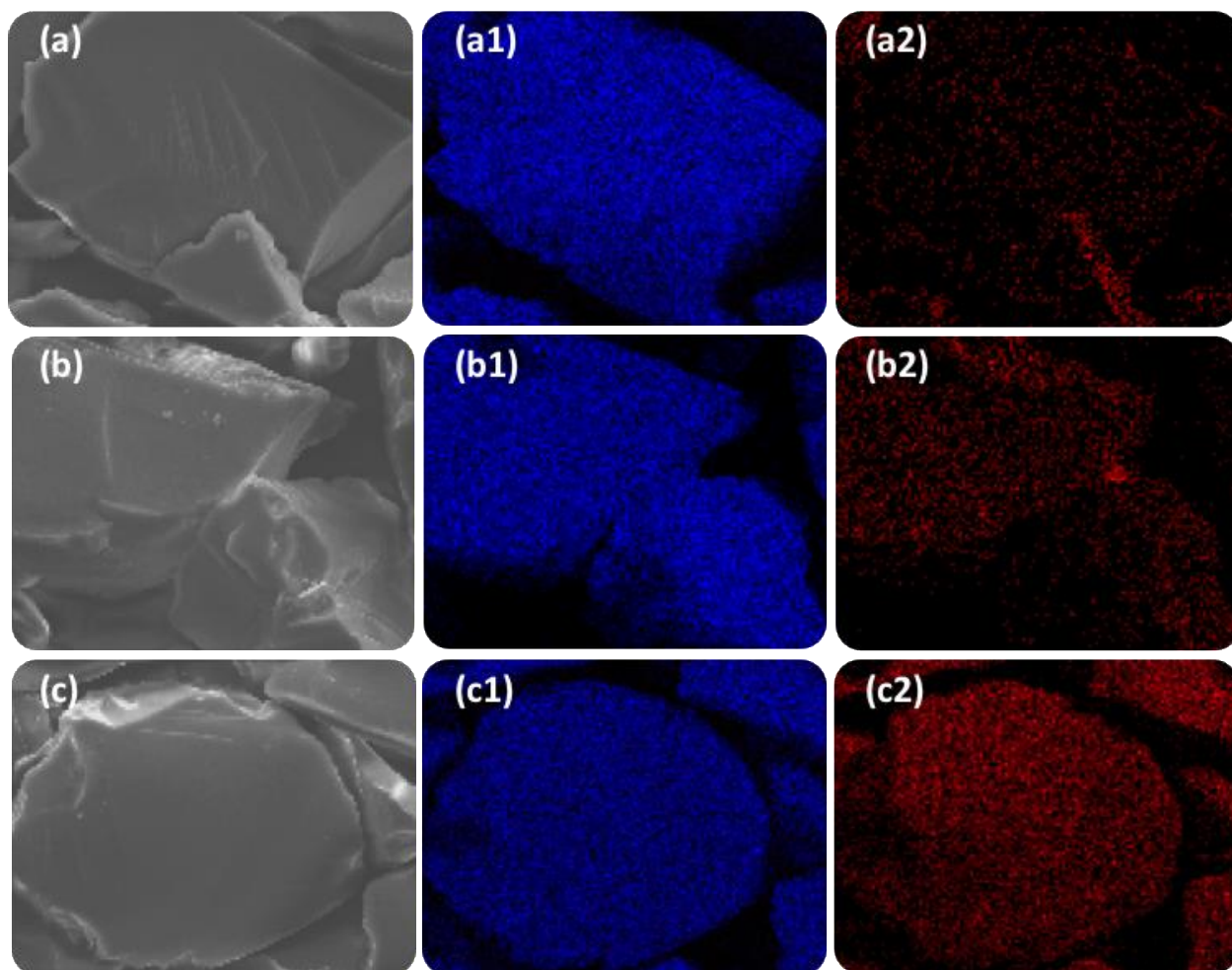


Figure 4.6. SEM images of (a) Si@NH₂, (b) Si@ACPA and (c) Si@PVP84-8h and corresponding SEM-EDX mappings for Si (indicated by «1», blue) and for N (indicated by «2», red) atoms.

XPS has been widely used to characterize the changes taking place on the outmost surface after physical or chemical treatments. The XPS survey wide scans of Si@NH₂, Si@ACPA initiator and grafted silica samples with different brush lengths are shown in Figure 4.7. In the survey scans, the quantitative elemental composition of each sample is also inserted in the graph. As seen in Figure 4.7, immobilization of ACPA to silica yields a distinct increase in N content. Then, its amount increases further by grafting. The O/C ratio, which was 1.58 before the grafting, decreased to 1.13 and 0.22, respectively, once GD increased from 1.9 % to 19.9 % as the surface has become poorer in oxygen due to carbon-rich structure of PVP. C1s core level spectra presented in Figure 4.8 clearly shows

the appearance of new C=O component at ca. 288.1 eV after immobilization of ACPA to silica surface. This peak becomes more apparent following the grafting and its intensity increases with GD as seen in Figure 4.8c.

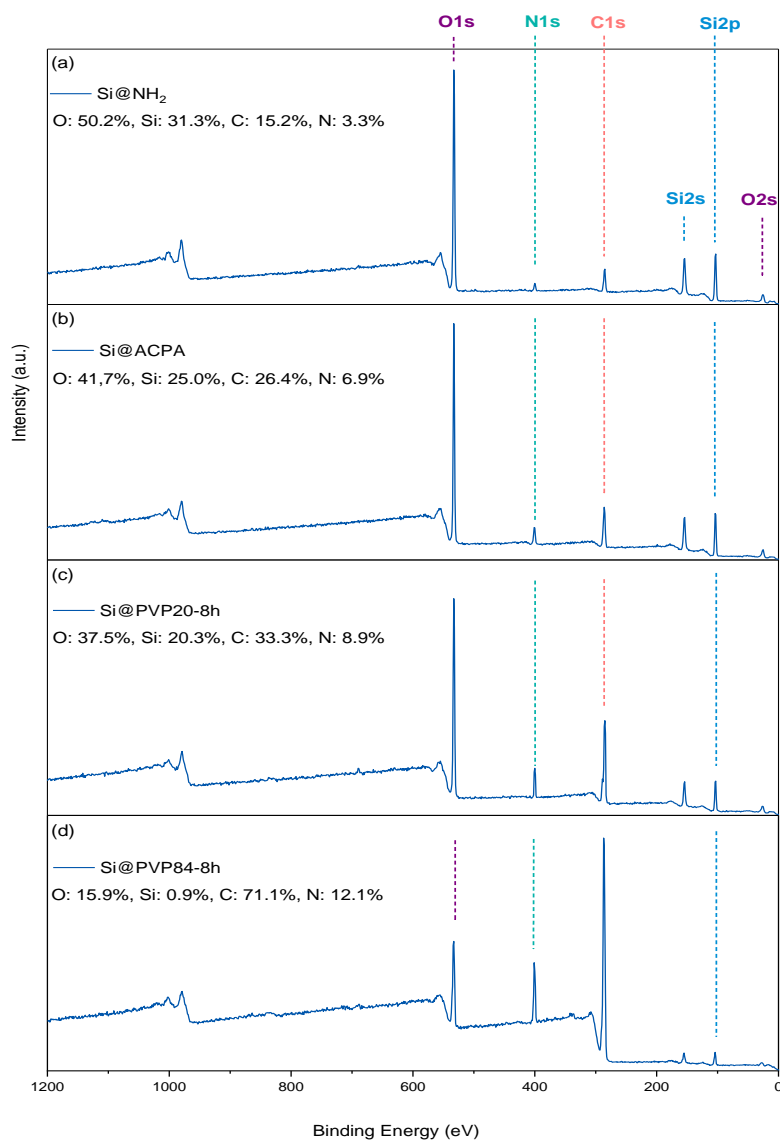


Figure 4.7. Survey wide-scan XPS spectra of (a) Si@NH₂, (b) Si@ACPA, (c) Si@PVP20-8h and (d) Si@PVP84-8h.

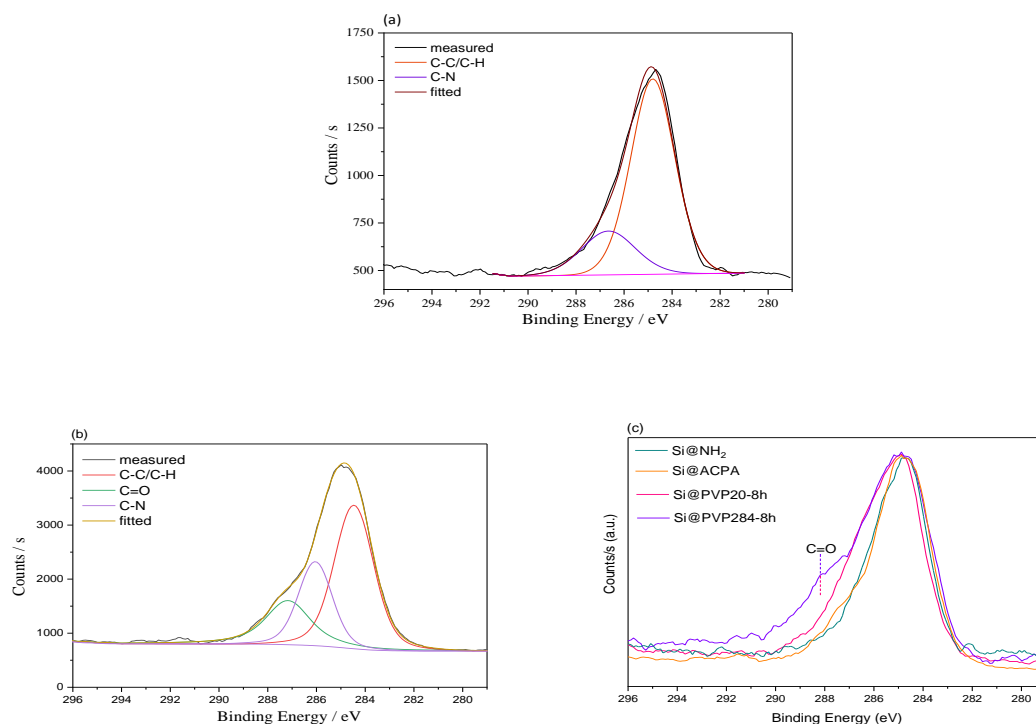


Figure 4.8. C1s spectra of (a) Si@NH₂, (b) Si@ACPA and (c) comparison of C1s spectra of various samples.

Irradiation by ionizing radiation such as gamma-rays has been widely used to create reductive medium for the preparation of metallic nanoparticles under eco-friendly conditions [4, 7, 146, 147]. This approach has been advantageous since it is effective, simple and does not require any chemical reducing agent. The radiolysis products of water mainly consist of oxidative ($\text{OH}\cdot$, $E_{\text{OH}\cdot/\text{H}_2\text{O}}^0 = +2.8$ V) and reductive ($\text{H}\cdot$, $E_{\text{H}\cdot/\text{H}_2\text{O}}^0 = -2.3$ V and hydrated electron, e_{aq}^- , $E_{\text{H}_2\text{O}/e_{\text{aq}}^-}^0 = -2.87$ V) species. Oxidative hydroxyl radicals can be eliminated using primary or secondary alcohols or formate ions as scavenger [1, 148]. Previous works mainly focus on using an alcohol in aqueous media for the synthesis of metal nanoparticles [11, 149–151]. Non-aqueous solvents such as methanol [152], 2-propanol [153] and supercritical ethane [154] also been used to form metal NPs under irradiation. We elaborated the effect of solvent on the γ -induced reduction of Pd(II) into Pd(0) NPs by employing water, EtOH and EtOH:water (40:60, v/v) mixture as the solvent. As can be seen in Figure 4.9, UV absorption spectrum of Pd(OAc)_{2(aq)} presents a broad band centered at ca. 280 nm corresponding to Pd(II) ions before the irradiation [155]. The intensity of this peak decreases significantly following the irradiation as a result of reduction of Pd(II) to zero-valent Pd as can be seen in the spectra of filtrates of Si@PVP-

PdNP samples. It is clear in Figure 4.9 that the reduction in EtOH and water is incomplete, as indicated from the Pd(II) ion peak still present at 280 nm. On the other hand, EtOH:water (40:60, v/v) mixture yielded almost a complete reduction of Pd(II) to zero-valent Pd NPs in solution.

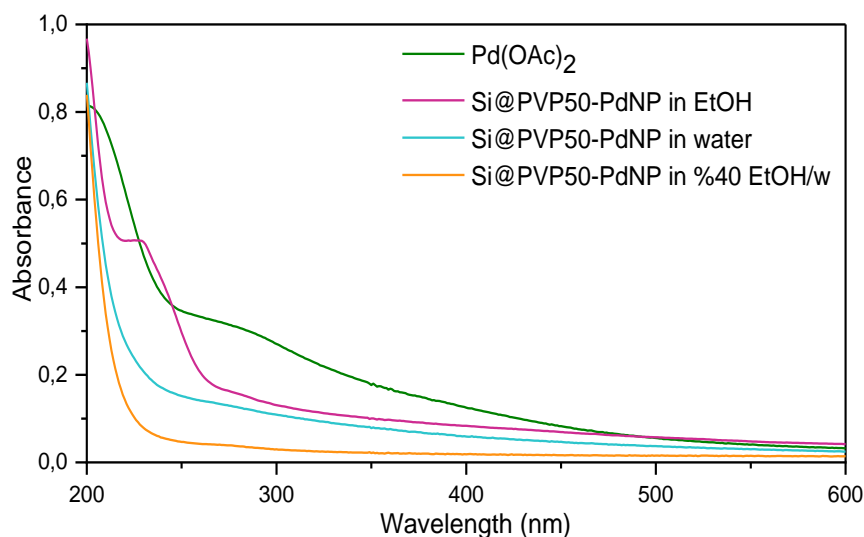


Figure 4.9. UV-vis absorption spectra of Pd(OAc)_{2(aq)} and filtrates of Si@PVP-Pd NP samples prepared in different solvents.

Dynamic light-scattering (DLS) technique was used for nanoparticles to estimate the average hydrodynamic diameter of Pd NPs or relative products prepared in different radiolytic conditions. Since the particle size distributions of Si@PVP filtrates presented in Figure 4.10 are bimodal or multimodal, average hydrodynamic diameter of each peak was individual calculated and given in Table 4.2. The DLS profile of Pd(OAc)₂ solution (0.45 mM in EtOH:water; 40:60, v/v mixture) irradiated in the absence of Si@PVP stabilizer appears as a unimodal peak with an average diameter of 333.8 nm as presented in Figure 4.10a and Table 4.2. This indicates that a cluster formation takes place in the absence of a stabilizer during the radiolytic reduction due to aggregation and dynamic intermolecular interactions. When Si@PVP50 stabilizer is added to the same solution, a distinct second peak corresponding to Pd NPs is observed at 31.4 nm (entry 2 in Table 4.2). These nanoparticles correspond to those that have passed into solution by leaking through the PVP shell, and are very significant as they demonstrate that PVP grafts are capable of forming and stabilizing nanoparticles despite being attached to a solid heterogeneous phase. Although a small amount of NPs with average size of 18 nm is also appeared in the solution irradiated in water alone, a broad peak corresponding to aggregated particles with

average size of 2910 nm is quite remarkable. When EtOH is employed as the solvent, a single peak centered at 1477 nm appeared indicating that the system had a high tendency to agglomerate and that nanoparticle formation could not be achieved (entry 4 in Table 4.2). When DLS results are evaluated together with UV-vis analysis, EtOH:water (40:60, v/v) mixture appeared as the most suitable solvent for the preparation of Pd NPs and hence employed in the rest of this study.

Table 4.2. DLS results of non-irradiated Pd(OAc)₂ and Si@PVP-PdNP prepared in different solvents and/or with different PVP lengths.

| Entry | Sample | Pk1 ^a | Pk2 ^b | Pk3 ^c |
|-------|--|------------------|------------------|------------------|
| | | d.nm | d.nm | d.nm |
| 1 | Pd(OAc) ₂ | - | 333.8 | - |
| 2 | Si@PVP50-PdNP in %40 EtOH/w (VP:Pd = 1:10) | 31.4 | 279.1 | - |
| 3 | Si@PVP50-PdNP in water (VP:Pd = 1:10) | 18.9 | 126.9 | 2910 |
| 4 | Si@PVP50-PdNP in EtOH (VP:Pd = 1:10) | - | - | 1477 |
| 5 | Si@PVP50-PdNP in %40 EtOH/w (VP:Pd = 1:1) | - | 304.9 | - |
| 6 | Si@PVP33-PdNP in %40 EtOH/w (VP:Pd = 1:10) | - | 190.7 | - |
| 7 | Si@PVP20-PdNP in %40 EtOH/w (VP:Pd = 1:10) | 60.9 | 362.6 | - |

^aStabilized NPs in nano-size region, ^bunstabilized aggregated particles with average size less than 400 nm, ^cunstabilized aggregated particles of micron size.

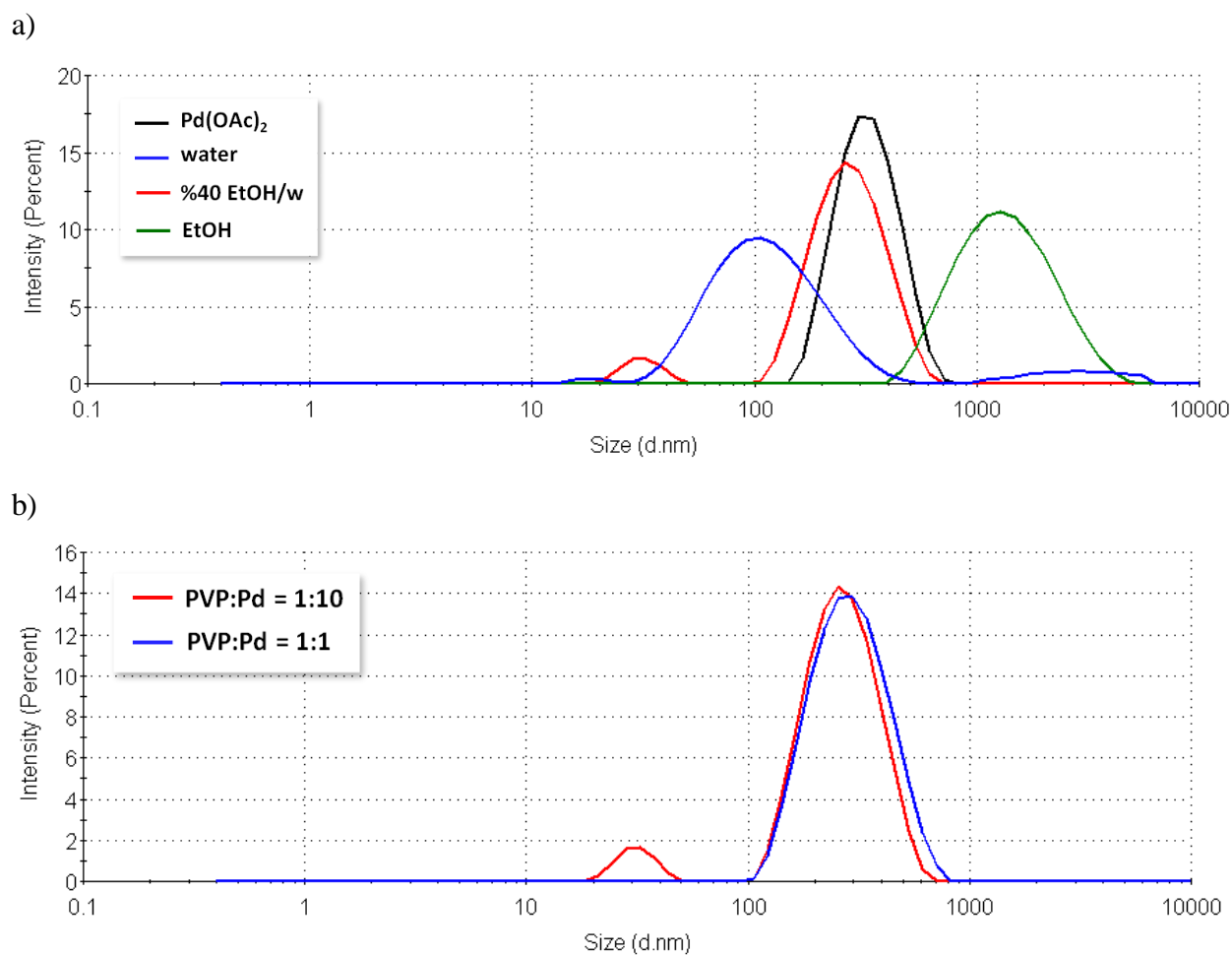


Figure 4.10. (a) DLS distribution of filtrates of Si@PVP50-PdNP prepared in ethanol (green), %40 EtOH/water (red), water (blue) and non-irradiated Pd(OAc)₂ solution in %40 EtOH/water (black). (b) DLS distribution of Si@PVP50-PdNP prepared with VP:Pd ratio as 1:1 (blue) and 1:10 (red).

The molar ratio between the precursor metal salt and stabilizing polymer significantly affects the nanoparticle formation [156]. We tested Pd:VP molar ratios of 1:1 and 1:10 and saw that no Pd NP was detectable in DLS for 1:1 mole ratio (entry 5 in Table 4.2) while a significant NP contribution was measured at 1:10 ratio as can be seen in Figure 4.10b. This shows that PVP stabilizer strongly promotes the formation of Pd NPs and its higher concentration offers a stronger stability to prevent the aggregation of nanoparticles. A high amount (frequency) of metal NPs within the stabilizing polymer matrix is desirable for the achievement of a high catalytic activity. Therefore, we chose 1:10 (Pd:VP) mol ratio for the rest of this study.

In order to topographically characterize the silica-based catalyst, Si@PVP50-PdNP specimen was selected as a representative and analyzed by AFM following to γ -irradiation. The specimen stored in acetone after irradiation was sonicated for 10 s, then leaved to rest for a while. Large Si@PVP50 particles precipitated, while the smaller ones remaining in solution were dropped on mica surface and analyzed by AFM. The height-based AFM image in Figure 4.11a clearly shows the irregularly shaped silica core. The PVP shell around this core barely appears in the height picture. The phase image in Figure 4.11b, on the other hand, clearly shows two distinct phases corresponding to silica microparticle as the core and PVP matrix as the grafted shell. The irregularity of the resultant core-shell microparticle derive from the random structure of silica is clearly reflected by the PVP shell, indicating a homogeneous coverage of the core. Small NPs around the silica microparticle correspond to Pd nanoparticles that leak from the PVP shell during the storage in acetone and the sonication process applied prior to AFM analysis.

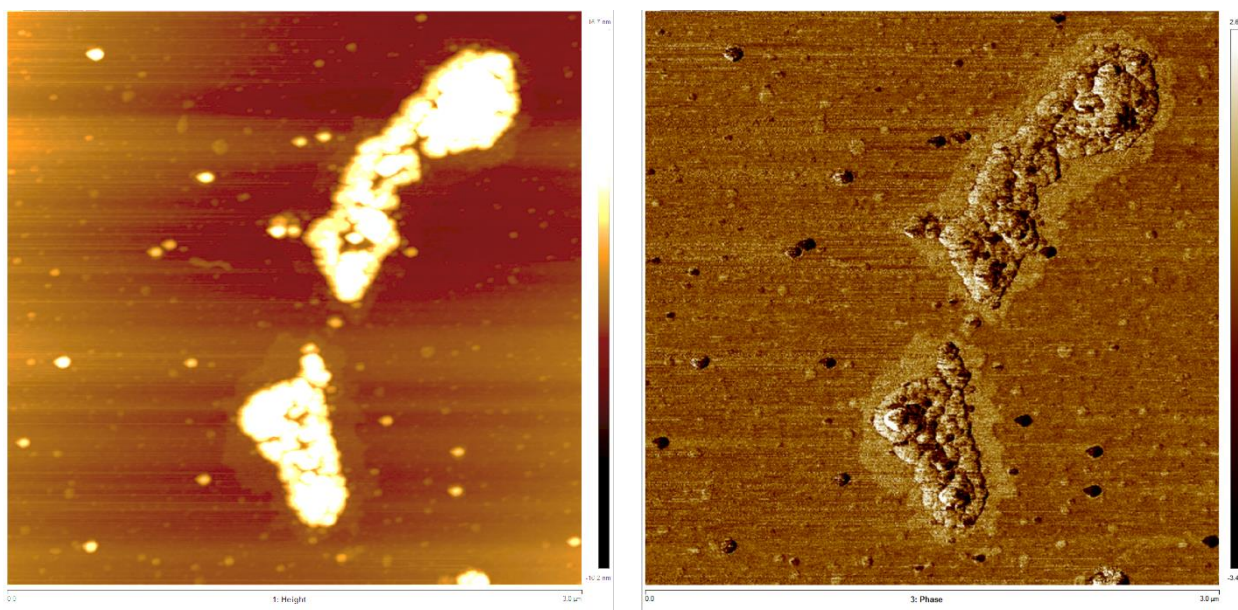
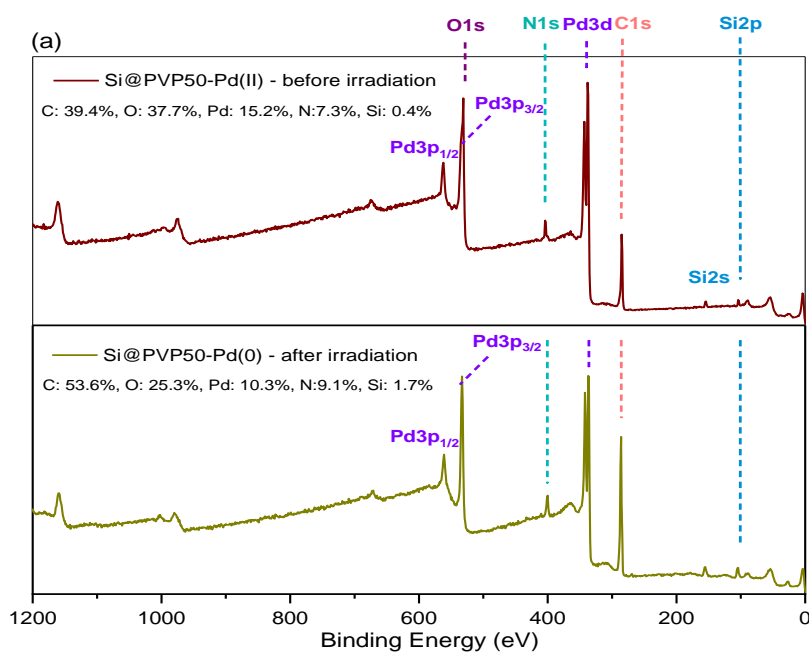


Figure 4.11. (a) AFM height and (b) phase images of Si@PVP50-PdNP: Irradiation dose: 10 kGy, 0.45 Mm Pd(OAc)₂ precursor solution in EtOH:water mixture (40:60, v/v).

Pd nanoparticles embedded in PVP shell cannot be seen in the AFM analysis. However, XPS data quantitatively displays the existence of Pd along with C, O, N and Si elements, as shown in Figure 4.12a. Pd element detected in XPS survey wide-scan of irradiated Si@PVP50-PdNP specimen corresponds to metallic Pd(0) NPs existing in ca. 10 nm of surface depth. Before irradiation, the characteristic peaks in high resolution XPS spectrum

of Pd 3d orbital appeared at binding energies of 336.5 eV and 341.9 eV could be attributed to Pd 3d_{5/2} and Pd3d_{3/2} (Figure 4.12b), respectively, which agrees well with the reported values for ionic Pd(II). The Pd 3d orbital spectrum of the irradiated sample presents the characteristic peaks centered at 335.3 eV and 340.5 eV correspond to 3d_{5/2} and 3d_{3/2} of metallic Pd(0), respectively. A small contribution of ionic Pd(II) appears in the spectrum of irradiated sample. The atomic ratio of Pd(II) to Pd(0) calculated from the peak areas was 1:12.7, suggesting that a very high degree of reduction occurs under irradiation, consequently leading to high Pd NP deposition into PVP shell.



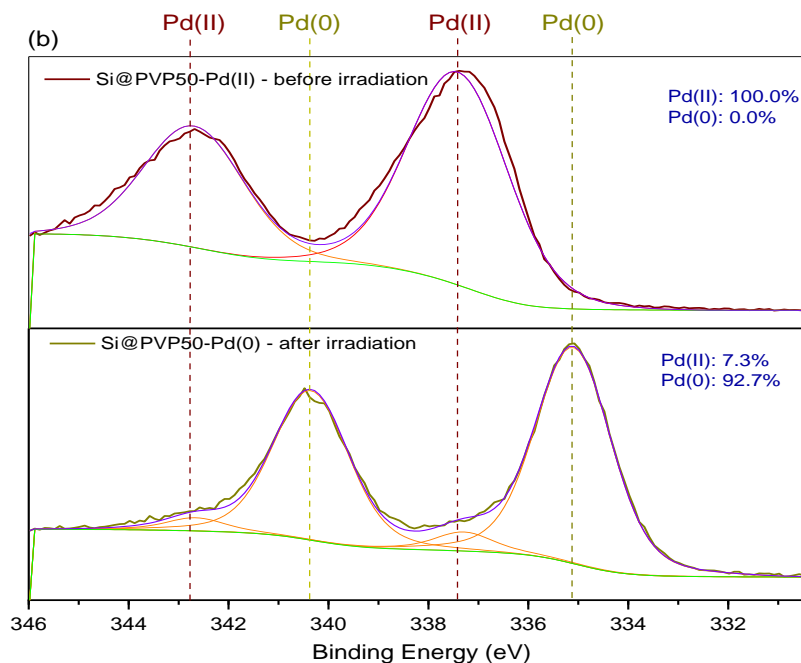


Figure 4.12. (a) Survey wide XPS scans and (b) Pd 3d core level scans of Pd(OAc)₂ absorbed PdSi@PVP50 sample before and after irradiation.

It is reported that the size of metallic nanoparticles strongly affects their catalytic activity. The main motivation of this study is to investigate the effect of chain length of the stabilizing polymer matrix attached to a surface on the formation of metal NPs and on their catalytic activity. We utilized RAFT polymerization to vary the lengths of PVP brushes and investigated the size of resultant NPs by DLS and TEM. Figure 4.13 shows the DLS distribution profile of Pd(OAc)₂ solution irradiated in the absence of Si@PVP and the filtrates of Si@PVP samples with different brush lengths (entries 1, 2, 6 and 7 in Table 4.2). The main peak appeared in all profiles corresponds to unstabilized Pd(OAc)₂ and its location varies indiscriminately. However, the peak arising from stabilized Pd shifts to smaller dimensions in the nano-size region as the molecular weight of the stabilizing polymer increases. This clearly indicates that the molecular weight of grafts attached to a substrate has a marked effect on the sizes of the resulting nanoparticles. We conducted TEM analysis to support this important finding.

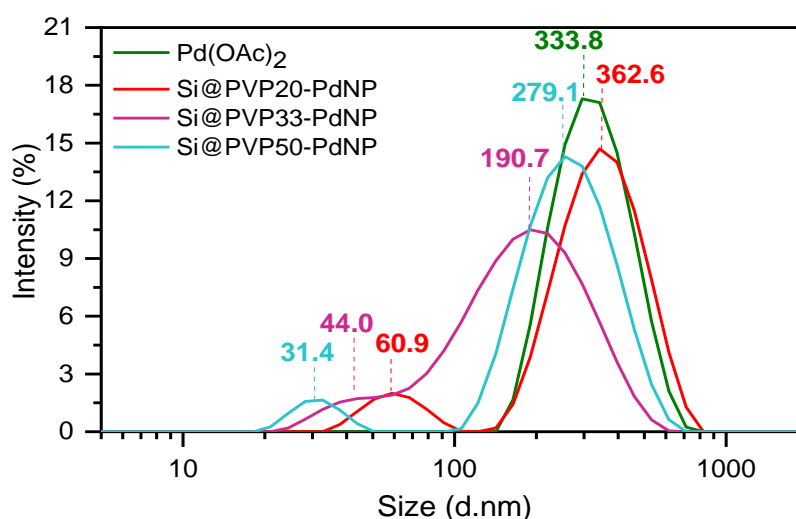


Figure 4.13. DLS distribution of Pd(OAc)₂ and filtrates of Si@PVP-PdNP samples with different PVP lengths following the irradiation (10 kGy, solvent:EtOH:water (40:60, v/v), Pd:VP=1:10)

Figure 4.14a exhibits the TEM image of a single silica particle at the core with a PVP shell decorated with Pd NPs. A closer look in Figure 4.14b reveals small NPs and some aggregated domains of larger ones with an average particle size of 7.8 ± 1.1 nm. When the target molecular weight of PVP grafts increase to 20 kDa from 50 kDa, the average size decreased to 4.6 ± 0.5 nm. Further increase in brush length decreased the average size to 3.0 ± 0.3 nm. Figure 4.14 also indicates that the shape and size of PdNPs became more uniform with the increase in molecular weight of PVP brushes. We, therefore, conclude that longer chains attached to silica offer more coercive environment against seed growth process and to some extent against aggregation too, yielding smaller NPs with narrower size distribution. These chains are likely to constitute more steric barrier, thus preventing the growing, thereby leading to the formation of nanoparticles smaller in size but larger in number. This claim is supported by the TEM-EDX mapping for Pd element across the TEM image in Figure 4.15a. As can be seen from the EDX mapping, Pd NPs propagate to each point of the PVP shell. There are small Pd seeds everywhere, not only in areas where larger particles are apparent. The dense areas are probably where nano-sized voids and free volumes exist in PVP shell.

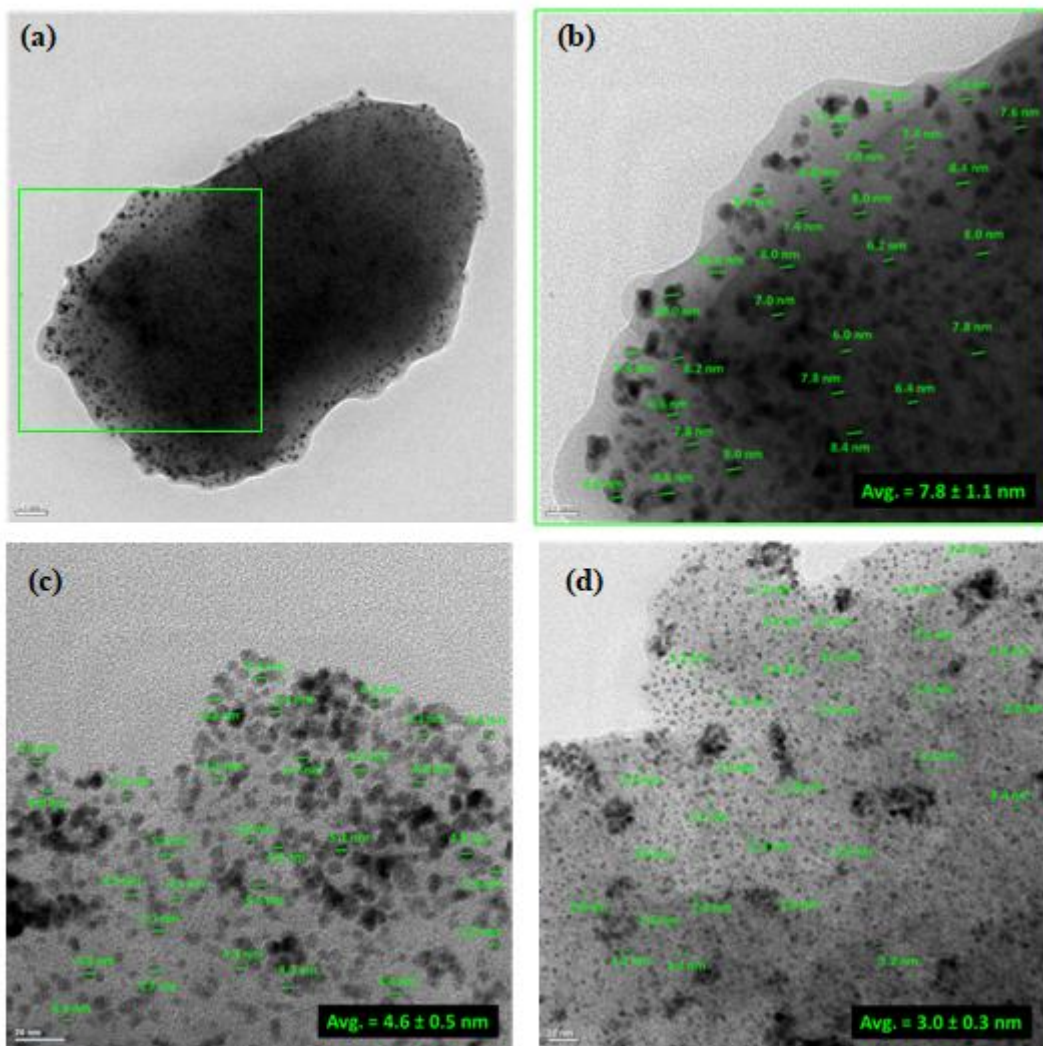


Figure 4.14. TEM images of Si@PVP20-PdNP (a, zoomed in b), Si@PVP50-PdNP (c) and Si@PVP84-PdNP (d).

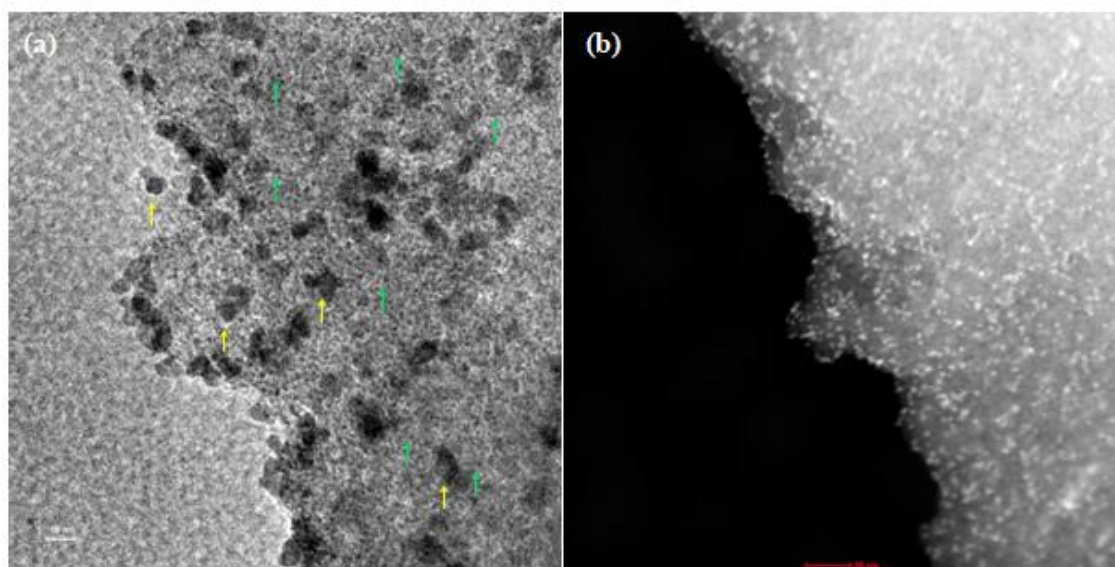


Figure 4.15. (a) TEM image of Si@PVP50-PdNP and (b) corresponding EDX mapping analysis for Pd element. Green arrows point small individual Pd seeds while yellow arrows show to denser areas where bigger particles are formed either by seed growth or aggregation.

Pd NP decorated Si@PVP samples with two different PVP brush length (SiPVP20@PdNP and SiPVP84@PdNP) were tested for their catalytic activity in hydrogenation of 4-NP. This reaction is widely regarded as a standard method to evaluate the reactivity of Pd species as potential catalysts [157–159]. Since 4-NP has a strong absorption peak at 400 nm, an easy and reliable measurement can be performed by following its reduction via UV-Vis spectroscopy, as presented in Figure 4.16a and 16b [146, 159]. As clearly seen from this figure, absorbance (A) of 4-NP peak decreases as the reaction proceeds. The reduction of 4-NP to 4-AP follows pseudo-first order kinetics because of excess amount of NaBH_4 as compared to 4-NP. Therefore, the kinetics of the reaction can be presented as $\ln(A_t/A_0) = -k t$, where k is the apparent first order rate constant, A_t and A_0 are the absorbance at specified time (t) and at $t=0$, respectively. As shown in Figure 4.16c, the relationship between $\ln(A_t/A_0)$ and reaction time (t) was close to linear and k was calculated to be 0.0311 min^{-1} for Si@PVP20-PdNP and 0.0423 min^{-1} for Si@PVP84-PdNP. A higher k value corresponds to a higher reaction rate, indicating a more efficiently catalyzed reaction. We, therefore, conclude that PVP grafts with higher molecular weights yield smaller NPs that exhibit a higher catalytic activity due to increased surface area [157, 160, 161].

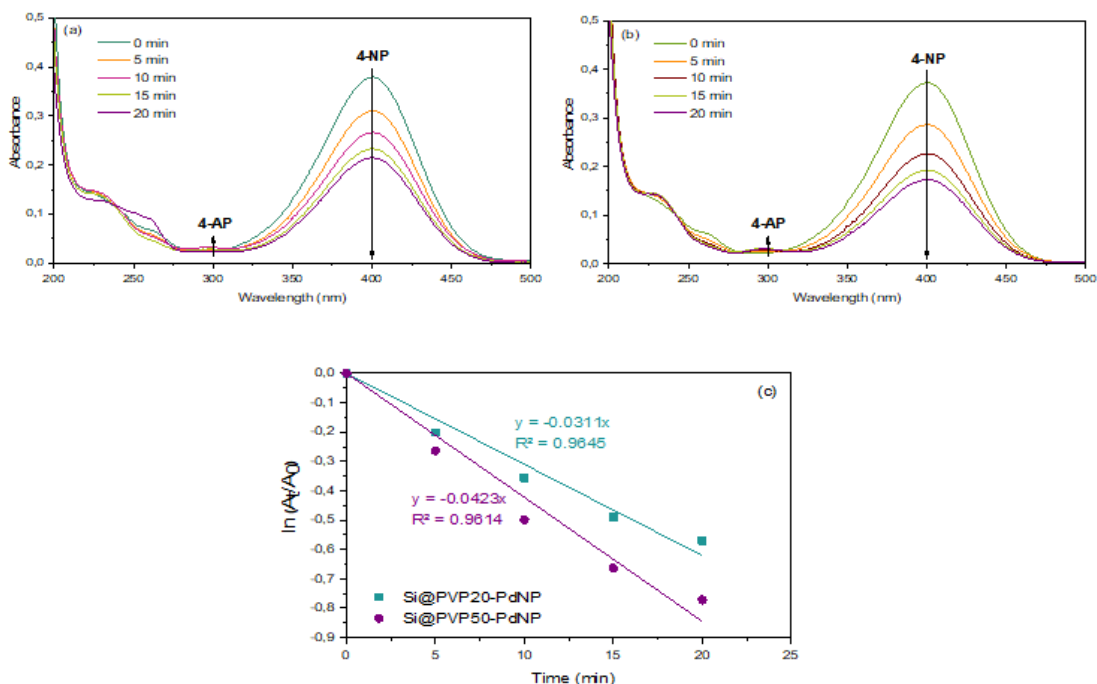


Figure 4.16. Time dependent UV-Vis absorption spectra for the reduction of 4-NP by NaBH₄ in the presence of (a) Si@PVP20-PdNP and (b) Si@PVP84-PdNP. Plot of ln(A_t/A₀) vs time (c) for the reduction of 4-NP by NaBH₄ in the presence of Si-PVP20@PdNP (■) and PVP84@PdNP (●).

The Si@PVP-Pd catalysts with brushes targeted to molecular weights of 20 kDa and 84 Kda were tested for their isolability and reusability in the reduction of 4-NP. After completion of the first reaction set, the catalysts were isolated by filtration and dried under vacuum at room temperature, then bottled in acetone. The bottled samples of Si@PVP-PdNP were filtered, dried, weighed and then reused in the next reaction set. The reduced amount of 4-NP (initial concentration: 3.91×10^{-6} M) per 5.0 mg of Si@PVP-Pd sample was calculated from the change in absorbance at 400 nm after completion of each reaction set. As can be seen in Figure 4.17, Si@PVP84-PdNP sample has shown less catalytic activity reduction compared to Si@PVP20-PdNP. At the end of 4th successive reaction run, Si@PVP84-PdNP retain 81.1 % of its initial activity, while Si@PVP20-PdNP fell behind with 73.5 %. One reason for the decrease in catalytic activity observed in both samples in subsequent runs may be attributed to the passivation of the surface of Pd NPs by increasing product, i.e. 4-AP, which decreases accessibility of active sites [162, 163].

However, the reason why the catalytic activity reduction differs significantly from one another between the samples cannot be explained by this. Here, we speculate that longer grafts are more effective in preventing NPs from leaking into the solution through the PVP shell, even if NPs are smaller in their presence, yet they allow the diffusion of reactants, resulting in more stable catalytic activity in subsequent reaction runs. On the other hand, short grafts are not sufficiently effective in preventing NP leakage, yielding a more prominent performance decrease in catalytic activity.

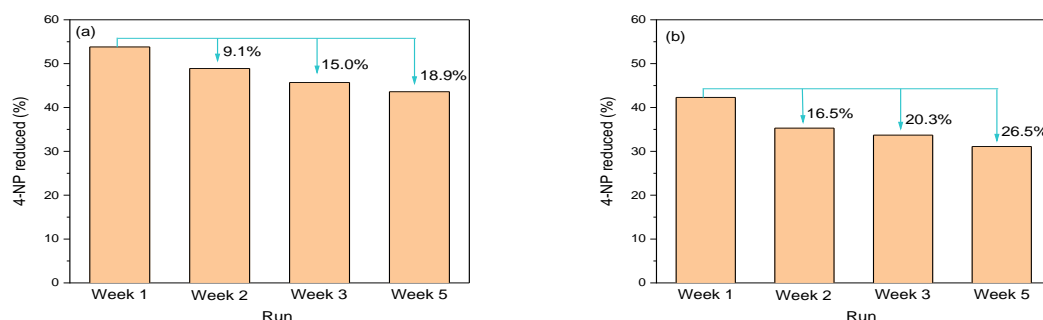


Figure 4.17. Catalytic performance in terms of ratio of reduced 4-NP obtained in the successive catalytic runs after isolation and redispersion of (a) Si@PVP84-PdNP, and (b) Si@PVP20-PdNP. $[4\text{-NP}]_0 = 3.91 \times 10^{-6}$ M, Si@PVP = 5.0 mg at 25.0 °C

5. CONCLUSION

The results obtained within the scope of this thesis can be summarized as follows;

- Poly(vinylpyrrolidone) (PVP) chains with different target molecular weights were grafted from silica core using RAFT-mediated graft polymerization in a controlled manner. From the results of various techniques, free radical initiator functionalized silica (Si@ACPA) and PVP grafted silica (Si@PVP) samples were found to be homogeneous and free from any spurious matter such as aggregated PVP domains.
- The grafted PVP shell was characterized by ATR-FTIR, TGA, SEC, XPS and TEM techniques. The PVP layer was then served as stabilizing matrix against the agglomeration of palladium (Pd) nanoparticles.
- Gamma-induced reduction was performed under eco-friendly conditions for the synthesis of Pd nanoparticles in the presence of Si@PVP stabilizer and the resultant nanoparticles were characterized by UV/Vis, DLS, XPS, AFM and TEM measurements.
- The results of DLS and TEM showed that the lengths of the grafted chains are an assistant factor to control the size and seed growth process of the synthesized nanoparticles. It has been revealed that increased molecular weight of PVP brushes sterically blocked the particle growth and yielded more small Pd nanoparticles rather than fewer large ones.
- Si@PVP-PdNP having different PVP lengths and Pd sizes were evaluated for their catalytic activity and reusability in the model reduction of 4-nitrophenol to 4-aminophenol. It has been found that longer grafts are more effective in preventing NPs from leaking into the solution through the PVP shell, even if nanoparticles are smaller in their presence, yet they allow the diffusion of reactants, resulting in more stable catalytic activity in repeated measurement cycles.
- On the other hand, short grafts were found to be less effective in preventing NP agglomeration and leakage. These findings are particularly important for

heterogeneous catalyst systems in that they show the effects of surface-bound polymeric stabilizers on NP formation and catalytic activity.

- The Si@PVP-PdNP catalysts could easily be isolated by filtration, bottled, reused and yet presented minor reduction in catalytic activity.
- We conclude that these findings are quite significant in terms of showing the effects of surface-bound polymeric stabilizers on the formation of NPs and their subsequent catalytic activity.

REFERENCES

- [1] A. Abedini, A. R. Daud, M. A. Abdul Hamid, N. Kamil Othman, and E. Saion, “A review on radiation-induced nucleation and growth of colloidal metallic nanoparticles,” *Nanoscale Res. Lett.*, vol. 8, no. 1, p. 474, Dec. **2013**.
- [2] J. Prakash, J. C. Pivin, and H. C. Swart, “Noble metal nanoparticles embedding into polymeric materials: From fundamentals to applications,” *Adv. Colloid Interface Sci.*, vol. 226, no. Pt B, pp. 187–202, Dec. **2015**.
- [3] M. Zahmakıran and S. Özkar, “Metal nanoparticles in liquid phase catalysis; from recent advances to future goals,” *Nanoscale*, vol. 3, no. 9, p. 3462, Sep. **2011**.
- [4] G. G. Flores-Rojas, F. López-Saucedo, and E. Bucio, “Gamma-irradiation applied in the synthesis of metallic and organic nanoparticles: A short review,” *Radiat. Phys. Chem.*, Aug. **2018**.
- [5] A. Henglein, “Physicochemical Properties of Small Metal Particles in Solution: ‘Microelectrode’ Reactions, Chemisorption, Composite Metal Particles, and the Atom-to-Metal Transition,” *J. Phys. Chem.*, vol. 97, no. 21, pp. 5457–5471, May **1993**.
- [6] B. I. Kharisov, O. V. Kharissova, and U. Ortiz Méndez, *Radiation synthesis of materials and compounds*. CRC Press, Taylor & Francis Group, **2013**.
- [7] J. L. Marignier, J. Belloni, M. O. Delcourt, and J. P. Chevalier, “Microaggregates of non-noble metals and bimetallic alloys prepared by radiation-induced reduction,” *Nature*, vol. 317, no. 6035, pp. 344–345, Sep. **1985**.
- [8] C. C. J. Seechurn, M. O. Kitching, T. J. Colacot, and V. Snieckus, “Palladium-Catalyzed Cross-Coupling: A Historical Contextual Perspective to the 2010 Nobel Prize,” *Angew. Chemie Int. Ed.*, vol. 51, no. 21, pp. 5062–5085, May **2012**.
- [9] A. Biffis, P. Centomo, A. Del Zotto, and M. Zecca, “Pd Metal Catalysts for Cross-Couplings and Related Reactions in the 21st Century: A Critical Review,” *Chem. Rev.*, vol. 118, no. 4, pp. 2249–2295, Feb. **2018**.
- [10] T. Iwasawa, M. Tokunaga, A. Y. Obora, and Y. Tsuji, “Homogeneous Palladium

- Catalyst Suppressing Pd Black Formation in Air Oxidation of Alcohols,” *J. Am. Chem. Soc.*, vol. 126, no. 21, **2004**.
- [11] M. Rakap, “The highest catalytic activity in the hydrolysis of ammonia borane by poly(N-vinyl-2-pyrrolidone)-protected palladium–rhodium nanoparticles for hydrogen generation,” *Appl. Catal. B Environ.*, vol. 163, pp. 129–134, Feb. **2015**.
- [12] M. Opanasenko, P. Stepnicka, and J. Cejka, “Heterogeneous Pd catalysts supported on silica matrices,” *RSC Adv.*, vol. 4, no. 110, pp. 65137–65162, Nov. **2014**.
- [13] N. Khodabakhsh, S. H. Maryam, D. Abdollah, P. Farhad, and H. N. M. Reza, “Modification of Silica Using Piperazine for Immobilization of Palladium Nanoparticles: A Study of Its Catalytic Activity as an Efficient Heterogeneous Catalyst for Heck and Suzuki Reactions,” *J. Iran. Chem. Soc.*, vol. 10, no. 3, pp. 527–534, Jan. **2013**.
- [14] F. P. da Silva, J. L. Fiorio, and L. M. Rossi, “Tuning the Catalytic Activity and Selectivity of Pd Nanoparticles Using Ligand-Modified Supports and Surfaces,” *ACS Omega*, vol. 2, no. 9, pp. 6014–6022, Sep. **2017**.
- [15] R. Liu, P. Liao, J. Liu, and P. Feng, “Responsive Polymer-Coated Mesoporous Silica as a pH-Sensitive Nanocarrier for Controlled Release,” *Langmuir*, vol. 27, no. 6, pp. 3095–3099, Mar. **2011**.
- [16] Y. Xia, Y. Xiong, B. Lim, and S. E. Skrabalak, “Shape-Controlled Synthesis of Metal Nanocrystals: Simple Chemistry Meets Complex Physics?,” *Angew. Chemie Int. Ed.*, vol. 48, no. 1, pp. 60–103, Jan. **2009**.
- [17] G. Chen *et al.*, “Interfacial electronic effects control the reaction selectivity of platinum catalysts,” *Nat. Mater.*, vol. 15, no. 5, pp. 564–569, May **2016**.
- [18] S. G. Kwon *et al.*, “Capping Ligands as Selectivity Switchers in Hydrogenation Reactions,” *Nano Lett.*, vol. 12, no. 10, pp. 5382–5388, Oct. **2012**.
- [19] M. Barsbay and O. Güven, “A short review of radiation-induced raft-mediated graft copolymerization: A powerful combination for modifying the surface properties of polymers in a controlled manner,” *Radiat. Phys. Chem.*, vol. 78, no. 12, pp. 1054–1059, Dec. **2009**.
- [20] M. Barsbay and O. Güven, “RAFT mediated grafting of poly (acrylic acid)(PAA) from polyethylene/polypropylene (PE/PP) nonwoven fabric via preirradiation,”

- Polymer (Guildf)*., vol. 54, no. 18, pp. 4838–4848, 2013.
- [21] M. Barsbay and O. Güven, “Grafting in confined spaces: Functionalization of nanochannels of track-etched membranes,” *Radiat. Phys. Chem.*, vol. 105, pp. 26–30, **2014**.
- [22] M. Barsbay, O. Güven, T. P. Davis, C. Barner-Kowollik, and L. Barner, “RAFT-mediated polymerization and grafting of sodium 4-styrenesulfonate from cellulose initiated via γ -radiation,” *Polymer (Guildf)*., vol. 50, no. 4, pp. 973–982, Feb. **2009**.
- [23] M. Barsbay, O. Güven, M. H. Stenzel, T. P. Davis, C. Barner-Kowollik, and L. Barner, “Verification of Controlled Grafting of Styrene from Cellulose via Radiation-Induced RAFT Polymerization,” *Macromolecules*, vol. 40, no. 20, pp. 7140–7147, Oct. **2007**.
- [24] G. Çelik, M. Barsbay, and O. Güven, “Towards new proton exchange membrane materials with enhanced performance via RAFT polymerization,” *Polym. Chem.*, vol. 7, no. 3, pp. 701–714, Jan. **2016**.
- [25] Y.-J. Song, M. Wang, X.-Y. Zhang, J.-Y. Wu, and T. Zhang, “Investigation on the role of the molecular weight of polyvinyl pyrrolidone in the shape control of high-yield silver nanospheres and nanowires,” *Nanoscale Res. Lett.*, vol. 9, no. 1, p. 17, Jan. **2014**.
- [26] H. Hirai and N. Yakura, “Protecting polymers in suspension of metal nanoparticles,” *Polym. Adv. Technol.*, vol. 12, no. 11–12, pp. 724–733, **2001**.
- [27] R. G. Shimmin, A. B. Schoch, and P. V Braun, “Polymer size and concentration effects on the size of gold nanoparticles capped by polymeric thiols,” *Langmuir*, vol. 20, no. 13, pp. 5613–20, Jun. **2004**.
- [28] C. M. Chan, A. T. Ko, and H. Hiraoka, “Polymer surface modification by plasmas and photons,” *Surf. Sci. Rep.*, vol. 24, no. 1–2, pp. 3–54, **1996**.
- [29] A. S. Hoffman, “Surface modification of polymers: Physical, chemical, mechanical and biological methods,” *Macromol. Symp.*, vol. 101, no. 1, pp. 443–454, Jan. **1996**.
- [30] R. N. Wahyu Nugroho, *Modification of Polymeric Particles via Surface Grafting for 3d Scaffold Design*. **2015**.
- [31] F. M. Michael, M. Khalid, R. Walvekar, H. Siddiqui, and A. B. Balaji, “Surface

- modification techniques of biodegradable and biocompatible polymers,” *Elsevier*, pp. 33–54, **2018**.
- [32] A. A. John *et al.*, “Review: physico-chemical modification as a versatile strategy for the biocompatibility enhancement of biomaterials,” *RSC Adv.*, vol. 5, no. 49, pp. 39232–39244, **2015**.
- [33] R. J. Young and P. A. L. Chapman, “Introduction to polymers,” *Polym. Int.*, vol. 27, no. 2, pp. 207–208, Jan. **1992**.
- [34] F. J. Xu, Z. H. Wang, and W. T. Yang, “Surface functionalization of polycaprolactone films via surface-initiated atom transfer radical polymerization for covalently coupling cell-adhesive biomolecules,” *Biomaterials*, vol. 31, no. 12, pp. 3139–3147, Apr. **2010**.
- [35] A. Bhattacharya and B. N. Misra, “Grafting: a versatile means to modify polymers: Techniques, factors and applications,” *Prog. Polym. Sci.*, vol. 29, no. 8, pp. 767–814, Aug. **2004**.
- [36] M. Ejaz, S. Yamamoto, K. Ohno, A. Y. Tsujii, and T. Fukuda, “Controlled Graft Polymerization of Methyl Methacrylate on Silicon Substrate by the Combined Use of the Langmuir–Blodgett and Atom Transfer Radical Polymerization Techniques,” *Macromolecules*, vol. 31, no. 17, pp. 5934–5936, **1998**.
- [37] X. Huang and M. J. Wirth, “Surface Initiation of Living Radical Polymerization for Growth of Tethered Chains of Low Polydispersity,” *Macromolecules*, vol. 32, no. 5, pp. 1694–1696, **1999**.
- [38] B. Z. And and W. J. Brittain, “Synthesis of Tethered Polystyrene-block-Poly(methyl methacrylate) Monolayer on a Silicate Substrate by Sequential Carbocationic Polymerization and Atom Transfer Radical Polymerization,” *J. Am. Chem. Soc.*, vol. 121, no. 14, pp. 3557–3558, **1999**.
- [39] M. Husseman *et al.*, “Controlled Synthesis of Polymer Brushes by ‘Living’ Free Radical Polymerization Techniques,” *Macromolecules*, vol. 32, pp. 1424–1431, **1999**.
- [40] Matyjaszewski Polymer Group, “Hybrid Brush Copolymers.” <https://www.cmu.edu/maty/materials/Nanostructured-materials/hybrid-brush-copolymers.html>. [Accessed: **22-May-2019**].

- [41] T. von W. And and T. E. Patten, "Preparation of Structurally Well-Defined Polymer–Nanoparticle Hybrids with Controlled/Living Radical Polymerizations," *J. Am. Chem. Soc.*, vol. 121, pp. 7409–7410, **1999**.
- [42] B. De Boer, H. K. Simon, M. P. L. Werts, E. W. Van Der Vegte, and G. Hadziioannou, "‘Living’ free radical photopolymerization initiated from surface-grafted iniferter monolayers," *Macromolecules*, vol. 33, no. 2, pp. 349–356, **2000**.
- [43] J. B. Kim, M. L. Bruening, and G. L. Baker, "Surface-initiated atom transfer radical polymerization on gold at ambient temperature," *Am. Chem. Soc. Polym. Prepr. Div. Polym. Chem.*, vol. 41, no. 2, p. 1300, **2000**.
- [44] C. Barner-Kowollik, *Handbook of RAFT polymerization*. Weinheim, Germany: Wiley-VCH, **2008**.
- [45] M. Shamsipur, J. Fasihi, and K. Ashtari, "Grafting of Ion-Imprinted Polymers on the Surface of Silica Gel Particles through Covalently Surface-Bound Initiators: A Selective Sorbent for Uranyl Ion," *Anal. Chem.*, vol. 79, no. 18, pp. 7116–7123, Sep. **2007**.
- [46] B. Zdyrko and I. Luzinov, "Polymer Brushes by the ‘Grafting to’ Method," *Macromol. Rapid Commun.*, vol. 32, no. 12, pp. 859–869, Jun. **2011**.
- [47] A. E. Müftüoğlu and Y. Yağcı, "Fotopolimerizasyon yöntemiyle çapraz bağlı ve aşırı kopolimerler hazırlanması," *itü*, vol. 3, no. 1, pp. 73–78, **2005**.
- [48] M. Asai, D. Zhao, and S. K. Kumar, "Role of Grafting Mechanism on the Polymer Coverage and Self-Assembly of Hairy Nanoparticles," *ACS Nano*, vol. 11, no. 7, pp. 7028–7035, Jul. **2017**.
- [49] M. Stamm, "Polymer Surface and Interface Characterization Techniques," in *Polymer Surfaces and Interfaces*, Berlin, Heidelberg: Springer Berlin Heidelberg, pp. 1–16, **2008**.
- [50] Z. Li, "Well-defined molecular brushes: Synthesis by a ‘grafting through’ strategy and self assembly into complicated hierarchical nanostructures Doctor of Philosophy," Washington University, **2011**.
- [51] M. Zhang and A. H. E. Müller, "Cylindrical polymer brushes," *J. Polym. Sci. Part A Polym. Chem.*, vol. 43, no. 16, pp. 3461–3481, Aug. **2005**.

- [52] J. Zhao, G. Mountrichas, G. Zhang, and S. Pispas, "Thermoresponsive Core–Shell Brush Copolymers with Poly(propylene oxide)- *block* -poly(ethylene oxide) Side Chains via a 'Grafting from' Technique," *Macromolecules*, vol. 43, no. 4, pp. 1771–1777, Feb. **2010**.
- [53] S. Edmondson and B. Zhu, "Applying ARGET ATRP to the Growth of Polymer Brush Thin Films by Surface-initiated Polymerization," *Aldrich Mater. Sci.*, pp. 12–14, **2012**.
- [54] H. Arslan, "Block and Graft Copolymerization by Controlled/Living Radical Polymerization Methods," *Polymerization*, pp. 279–287, Dec. **2012**.
- [55] V. Mishra and R. Kumar, "Living Radical Polymerization: A Review," vol. 56, pp. 141–176, **2012**.
- [56] G. Moad, E. Rizzardo, and S. H. Thang, "Radical addition–fragmentation chemistry in polymer synthesis," *Polymer*, vol. 49, no. 5, pp. 1079–1131, Mar. **2008**.
- [57] R. H. Grubbs and W. Tumas, "Polymer synthesis and organotransition metal chemistry," *Science*, vol. 243, no. 4893, pp. 907–15, Feb. 1989.
- [58] R. Ranjan, "Surface Modification of Silica Nanoparticles, Doctor of Philosophy," University of Akron, **2008**.
- [59] K. Matyjaszewski and J. Spanswick, "Controlled/living radical polymerization," *Mater. Today*, vol. 8, no. 3, pp. 26–33, Mar. **2005**.
- [60] K. Matyjaszewski, Y. Gnanou, and L. Leibler, *Macromolecular engineering : precise synthesis, materials properties, applications*. Wiley-VCH, **2007**.
- [61] C. D. Craver and C. E. Carraher, *Applied polymer science : 21st century*. Elsevier, **2000**.
- [62] H. Mark, "Carbanions living polymers and electron transfer processes. M. Szwarc, ed. John Wiley & Sons, Inc. New York, 1968.," *J. Appl. Polym. Sci.*, vol. 14, no. 3, pp. 859–859, Mar. **1970**.
- [63] H. L. Hsieh and R. P. Quirk, "Anionic polymerization : principles and practical applications." <https://trove.nla.gov.au/work/21907558?selectedversion=NBD12134956>. [Accessed: **22-May-2019**].
- [64] K. (Krzysztof) Matyjaszewski, *Cationic polymerizations : mechanisms, synthesis*,

- and applications*. Marcel Dekker, **1996**.
- [65] O. W. Webster, "Living Polymerization Methods," *Science*, vol. 251, no. 4996, pp. 887–893, Feb. **1991**.
- [66] K. Matyjaszewski and T. P. Davis, *Handbook of radical polymerization*. Wiley-Interscience, **2002**.
- [67] V. Coessens and K. Matyjaszewski, "Synthesis of polymers with amino end groups by atom transfer radical polymerization," *J. Macromol. Sci. Part A*, vol. 36, no. 5–6, pp. 811–826, Jun. **1999**.
- [68] K. Matyjaszewski, "Non-living Cationic Polymerization of Alkenes," *Polym. Int.*, vol. 35, pp. 1–26, **1994**.
- [69] T. E. Patten and K. Matyjaszewski, "Atom Transfer Radical Polymerization and the Synthesis of Polymeric Materials," *Adv. Mater.*, vol. 10, no. 12, pp. 901–915, Aug. **1998**.
- [70] H. R. Kricheldorf, O. Nuyken, and G. Swift, *Handbook of Polymer Synthesis: Second Edition*. New York, **2005**.
- [71] T. E. Patten and K. Matyjaszewski, "Copper(I)-Catalyzed Atom Transfer Radical Polymerization," *Acc. Chem. Res.*, vol. 32, no. 10, pp. 895–903, **1999**.
- [72] E. Khosravi and T. Szymanska-Buzar, "Ring Opening Metathesis Polymerisation and Related Chemistry." https://www.researchgate.net/publication/282444950_Ring_Opening_Metathesis_Polymerisation_and_Related_Chemistry. [Accessed: **26-May-2019**].
- [73] K. Matyjaszewski, M. J. Ziegler, S. V. Arehart, D. Greszta, and T. Pakula, "Gradient copolymers by atom transfer radical copolymerization," *J. Phys. Org. Chem.*, vol. 13, no. 12, pp. 775–786, **2000**.
- [74] W. Jakubowski, A. K. Min, and K. Matyjaszewski, "Activators Regenerated by Electron Transfer for Atom Transfer Radical Polymerization of Styrene," *Macromolecules*, vol. 39, no. 1, pp. 39–45, **2005**.
- [75] K. Matyjaszewski *et al.*, "Diminishing catalyst concentration in atom transfer radical polymerization with reducing agents," *Proc. Natl. Acad. Sci.*, vol. 103, no. 42, pp. 15309–15314, Oct. **2006**.

- [76] W. Jakubowski *et al.*, “Contents Full Papers Polystyrene with Improved Chain-End Functionality and Higher Molecular Weight by ARGET ATRP Conductive Polymer Electrolytes Derived from Poly(norbornene)s with Pendant Ionic Imidazolium Moieties Novel Amphiphilic Styrene-Based Block C,” *Macromol. Chem. Phys.*, vol. 209, pp. 3–8, **2008**.
- [77] K. Matyjaszewski *et al.*, “Role of Cu⁰ in Controlled/‘Living’ Radical Polymerization,” *Macromolecules*, vol. 40, no. 22, pp. 7795–7806, **2007**.
- [78] F. E. McDonald, “Alkynolendo-Cyclo isomerizations and Conceptually Related Transformations,” *Chem. - A Eur. J.*, vol. 5, no. 11, pp. 3103–3106, Nov. **1999**.
- [79] H. Dong and K. Matyjaszewski, “Arget ATRP of 2-(Dimethylamino)ethyl Methacrylate as an Intrinsic Reducing Agent,” *Macromolecules*, vol. 41, no. 19, pp. 6868–6870, Oct. **2008**.
- [80] V. Mittal, N. B. Matsko, A. Butté, and M. Morbidelli, “Synthesis of temperature responsive polymer brushes from polystyrene latex particles functionalized with ATRP initiator,” *Eur. Polym. J.*, vol. 43, no. 12, pp. 4868–4881, Dec. **2007**.
- [81] K. Matyjaszewski and S. G. Gaynor, “Free Radical Polymerization,” *Appl. Polym. Sci. 21st Century*, pp. 929–977, Jan. **2000**.
- [82] “Polymerization process and polymers produced thereby,” 11-Jul-1984. <https://patents.google.com/patent/US4581429A/en>. [Accessed: **26-May-2019**].
- [83] J. Nicolas, Y. Guillaneuf, C. Lefay, D. Bertin, D. Gigmes, and B. Charleux, “Nitroxide-mediated polymerization,” *Prog. Polym. Sci.*, vol. 38, no. 1, pp. 63–235, Jan. **2013**.
- [84] “Block copolymer synthesis using a commercially available nitroxide mediated radical polymerization (NMP) initiator.” https://www.researchgate.net/publication/286782734_Block_copolymer_synthesis_using_a_commercially_available_nitroxide-mediated_radical_polymerization_NMP_initiator. [Accessed: **26-May-2019**].
- [85] H. Fischer, “The Persistent Radical Effect: A Principle for Selective Radical Reactions and Living Radical Polymerizations,” *Chem. Rev.*, vol. 101, no. 12, pp. 3581–3610, **2001**.
- [86] M. K. Georges, R. P. N. Veregin, P. M. Kazmaier, and G. K. Hamer, “Narrow molecular weight resins by a free-radical polymerization process,” *Macromolecules*,

- vol. 26, no. 11, pp. 2987–2988, May **1993**.
- [87] A. Nilsen and R. Braslau, “Nitroxide decomposition: Implications toward nitroxide design for applications in living free-radical polymerization,” *J. Polym. Sci. Part A Polym. Chem.*, vol. 44, no. 2, pp. 697–717, **2006**.
- [88] R. B. Grubbs, “Nitroxide-Mediated Radical Polymerization: Limitations and Versatility,” *Polym. Rev.*, vol. 51, no. 2, pp. 104–137, Apr. **2011**.
- [89] M. Hosseini and A. S. H. Makhlof, *Industrial Applications for Intelligent Polymers and Coatings*. Cham: Springer International Publishing, **2016**.
- [90] K. Matyjaszewski and N. V. Tsarevsky, “Nanostructured functional materials prepared by atom transfer radical polymerization,” *Nat. Chem.*, vol. 1, no. 4, pp. 276–288, Jul. **2009**.
- [91] M. Ouchi, T. Terashima, and M. Sawamoto, “Transition Metal-Catalyzed Living Radical Polymerization: Toward Perfection in Catalysis and Precision Polymer Synthesis,” *Chem. Rev.*, vol. 109, no. 11, pp. 4963–5050, Nov. **2009**.
- [92] M. Destarac, D. Charmot, X. Franck, and S. Z. Zard, “Dithiocarbamates as universal reversible addition-fragmentation chain transfer agents,” *Macromol. Rapid Commun.*, vol. 21, no. 15, pp. 1035–1039, Oct. **2000**.
- [93] R. T. A. Mayadunne *et al.*, “Living Polymers by the Use of Trithiocarbonates as Reversible Addition-Fragmentation Chain Transfer (RAFT) Agents: ABA Triblock Copolymers by Radical Polymerization in Two Steps,” *Macromolecules*, vol. 33, no. 2, pp. 243–245, **2000**.
- [94] R. F. And and A. Ajayaghosh, “Minimization of Homopolymer Formation and Control of Dispersity in Free Radical Induced Graft Polymerization Using Xanthate Derived Macro-photoinitiators,” *Macromolecules*, vol. 33, no. 13, pp. 4699–4704, **2000**.
- [95] G. Moad, E. Rizzardo, and S. H. Thang, “Toward Living Radical Polymerization,” *Acc. Chem. Res.*, vol. 41, no. 9, pp. 1133–1142, Sep. **2008**.
- [96] J. Chiefari *et al.*, “Living Free-Radical Polymerization by Reversible Addition-Fragmentation Chain Transfer: The RAFT Process,” *Macromolecules*, vol. 31, pp. 5559–5562, **1998**.

- [97] D. A. Shipp, "Living Radical Polymerization: Controlling Molecular Size and Chemical Functionality in Vinyl Polymers," *J. Macromol. Sci. Part C Polym. Rev.*, vol. 45, no. 2, pp. 171–194, Apr. **2005**.
- [98] J. Chiefari *et al.*, "Thiocarbonylthio Compounds (SC(Z)S–R) in Free Radical Polymerization with Reversible Addition-Fragmentation Chain Transfer (RAFT Polymerization). Effect of the Activating Group Z," *Macromolecules*, vol. 36, no. 7, pp. 2273–2283, **2003**.
- [99] G. Moad, Y. K. Chong, A. Postma, E. Rizzardo, and S. H. Thang, "Advances in RAFT polymerization: the synthesis of polymers with defined end-groups," *Polymer (Guildf)*, vol. 46, no. 19, pp. 8458–8468, Sep. **2005**.
- [100] R. T. A. Mayadunne, J. Jeffery, A. Graeme Moad, and Ezio Rizzardo, "Living Free Radical Polymerization with Reversible Addition–Fragmentation Chain Transfer (RAFT Polymerization): Approaches to Star Polymers," *Macromolecules*, vol. 36, no. 5, pp. 1505–1513, **2003**.
- [101] S. H. Thang, (Bill)Y.K. Chong, R. T. A. Mayadunne, G. Moad, and E. Rizzardo, "A novel synthesis of functional dithioesters, dithiocarbamates, xanthates and trithiocarbonates," *Tetrahedron Lett.*, vol. 40, no. 12, pp. 2435–2438, Mar. **1999**.
- [102] R. T. A. *et al.*, *Macromolecules.*, vol. 33, no. 2. American Chemical Society, **1968**.
- [103] X. Tian, J. Ding, B. Zhang, F. Qiu, X. Zhuang, and Y. Chen, "Recent advances in RAFT polymerization: Novel initiation mechanisms and optoelectronic applications," *Polymers (Basel)*, vol. 10, no. 3, **2018**.
- [104] I. W. Hamley, *Developments in block copolymer science and technology*. J. Wiley, **2004**.
- [105] D. J. Keddie, G. Moad, E. Rizzardo, and S. H. Thang, "RAFT Agent Design and Synthesis," *Macromolecules*, vol. 45, no. 13, pp. 5321–5342, Jul. **2012**.
- [106] S. H. Thang, (Bill)Y.K. Chong, R. T. A. Mayadunne, G. Moad, and E. Rizzardo, "A novel synthesis of functional dithioesters, dithiocarbamates, xanthates and trithiocarbonates," *Tetrahedron Lett.*, vol. 40, no. 12, pp. 2435–2438, Mar. **1999**.
- [107] D. Taton, A.-Z. Wilczewska, and M. Destarac, "Direct Synthesis of Double Hydrophilic Statistical Di- and Triblock Copolymers Comprised of Acrylamide and Acrylic Acid Units via the MADIX Process," *Macromol. Rapid Commun.*, vol. 22,

- no. 18, p. 1497, Dec. **2001**.
- [108] J. Loiseau *et al.*, “Synthesis and Characterization of Poly(acrylic acid) Produced by RAFT Polymerization. Application as a Very Efficient Dispersant of CaCO₃, Kaolin, and TiO₂,” *Macromolecules*, vol. 36, no. 9, pp. 3066–3077, **2003**.
- [109] J. J. Grodzinski, *Living and Controlled Polymerization: Synthesis, Characterization, and Properties of the Respective Polymers and Copolymers*. New York, **2006**.
- [110] B. Ray *et al.*, “Synthesis of Isotactic Poly(N-isopropylacrylamide) by RAFT Polymerization in the Presence of Lewis Acid,” *Macromolecules*, vol. 36, no. 3, pp. 543–545, **2003**.
- [111] M. Yin, *Synthesis and Controlled Radical Polymerization of Multifunctional Monomers*. Dresden, **2004**.
- [112] G. Çelik, “Poli(etilen-alt-tetrafloroetilen) (ETFE) Ardışık Kopolimer Filmine Raft Yöntemi ve Radyasyon Kullanılarak Stiren Aşılması ve Yakıt Pili Membranı Hazırlanması,” Hacettepe Üniversitesi, **2013**.
- [113] W. C. Wang, K. G. Neoh, and E. T. Kong, “Surface functionalization of Fe₃O₄ magnetic nanoparticles via RAFT-mediated graft polymerization,” *Macromol. Rapid Commun.*, vol. 27, no. 19, pp. 1665–1669, **2006**.
- [114] A. N. Shipway and I. Willner, “Nanoparticles as structural and functional units in surface-confined architectures,” *Chem. Commun.*, no. 20, pp. 2035–2045, Oct. **2001**.
- [115] K. L. Mittal, *Silanes and Other Coupling Agents*. Boston, **2009**.
- [116] C. Sha *et al.*, “Total Synthesis of (–)Dendrobine via α -Carbonyl Radical Cyclization,” *Langmuir*, vol. 119, no. 18, pp. 4130–4135, **1997**.
- [117] T. Yonezawa, A. Kuniko Imamura, and Nobuo Kimizuka, “Direct Preparation and Size Control of Palladium Nanoparticle Hydrosols by Water-Soluble Isocyanide Ligands,” *Langmuir*, vol. 17, no. 16, pp. 4701–4703, **2001**.
- [118] M. M. Demir *et al.*, “Palladium Nanoparticles by Electrospinning from Poly(acrylonitrile-co-acrylic acid)-PdCl₂ Solutions. Relations between Preparation Conditions, Particle Size, and Catalytic Activity,” *Macromolecules*, vol. 37, no. 5, pp. 1787–1792, **2004**.
- [119] H. Thiele and H. von Lavern, “Synthetic protective colloids,” *J. Colloid Sci.*, vol.

- 20, no. 7, pp. 679–694, Sep. **1965**.
- [120] S. V. Jadhav *et al.*, “Studies on colloidal stability of PVP-coated LSMO nanoparticles for magnetic fluid hyperthermia,” *New J. Chem.*, vol. 37, no. 10, p. 3121, Sep. **2013**.
- [121] G. Lu *et al.*, “Imparting functionality to a metal–organic framework material by controlled nanoparticle encapsulation,” *Nat. Chem.*, vol. 4, no. 4, pp. 310–316, Apr. **2012**.
- [122] H. Kung, “Applied Catalysis A: General,” *Sci. Direct*, vol. 482, pp. 1–406.
- [123] M. Bahadory, “Synthesis of noble metal nanoparticles,” *Mater. Sci. Eng. C*, vol. 22, no. August, p. 204, **2008**.
- [124] R. Si, Y.-W. Zhang, L.-P. You, and C.-H. Yan, “Self-Organized Monolayer of Nanosized Ceria Colloids Stabilized by Poly(vinylpyrrolidone),” *J. Phys. Chem. B*, vol. 110, no. 12, pp. 5994–6000, Mar. **2006**.
- [125] W. A. Al-Saidi, H. Feng, and K. A. Fichthorn, “Adsorption of Polyvinylpyrrolidone on Ag Surfaces: Insight into a Structure-Directing Agent,” *Nano Lett.*, vol. 12, no. 2, pp. 997–1001, Feb. **2012**.
- [126] “Polyvinylpyrrolidone - an overview,” *Science Direct*. <https://www.sciencedirect.com/topics/agricultural-and-biological-sciences/polyvinylpyrrolidone>. [Accessed: **27-May-2019**].
- [127] N. Gaponik *et al.*, “Thiol-Capping of CdTe Nanocrystals: An Alternative to Organometallic Synthetic Routes,” *J. Phys. Chem. B*, vol. 106, no. 29, pp. 7177–7185, **2002**.
- [128] T. K. Sau, A. L. Rogach, F. Jäckel, T. A. Klar, and J. Feldmann, “Properties and Applications of Colloidal Nonspherical Noble Metal Nanoparticles,” *Adv. Mater.*, vol. 22, no. 16, pp. 1805–1825, Apr. **2010**.
- [129] C. Burda, X. Chen, R. Narayanan, and M. A. El-Sayed, “Chemistry and Properties of Nanocrystals of Different Shapes,” *Chem. Rev.*, vol. 105, no. 4, pp. 1025–1102, Apr. **2005**.
- [130] R. Ameloot *et al.*, “Metal-Organic Framework Single Crystals as Photoactive Matrices for the Generation of Metallic Microstructures,” *Adv. Mater.*, vol. 23, no.

- 15, pp. 1788–1791, Apr. **2011**.
- [131] A. G. Chmielewski, D. K. Chmielewska, J. Michalik, and M. H. Sampa, “Prospects and challenges in application of gamma, electron and ion beams in processing of nanomaterials,” *Nucl. Instruments Methods Phys. Res. Sect. B Beam Interact. with Mater. Atoms*, vol. 265, no. 1, pp. 339–346, Dec. **2007**.
- [132] A. Henglein and D. Meisel, “Radiolytic Control of the Size of Colloidal Gold Nanoparticles,” *Langmuir*, vol. 14, no. 26, pp. 7392–7396, **1998**.
- [133] H. G. Elias, *Macromolecules: Volume 2: Synthesis, Materials, and Technology*. New York, **1984**.
- [134] “What is Radiation? – Mission to Mars.” <https://sites.duke.edu/missiontomars/the-mission/radiation/what-is-radiation/>. [Accessed: **27-May-2019**].
- [135] J. Belloni, M. Mostafavi, H. Remita, J.-L. Marignier, and M.-O. Delcourt, “Radiation-induced synthesis of mono- and multi-metallic clusters and nanocolloids,” *New J. Chem.*, vol. 22, no. 11, pp. 1239–1255, Jan. **1998**.
- [136] H. Remita and S. Remita, “Metal Clusters and Nanomaterials: Contribution of Radiation Chemistry,” in *Recent Trends in Radiation Chemistry*, World Scientific, pp. 347–383, **2010**.
- [137] H. A. Schwarz and R. W. Dodson, “Reduction potentials of CO₂- and the alcohol radicals,” *J. Phys. Chem.*, vol. 93, no. 1, pp. 409–414, Jan. **1989**.
- [138] J. Belloni, “Nucleation, growth and properties of nanoclusters studied by radiation chemistry: Application to catalysis,” *Catal. Today*, vol. 113, no. 3–4, pp. 141–156, Apr. **2006**.
- [139] K.-P. Lee, A. I. Gopalan, P. Santhosh, S. H. Lee, and Y. C. Nho, “Gamma radiation induced distribution of gold nanoparticles into carbon nanotube-polyaniline composite,” *Compos. Sci. Technol.*, vol. 67, no. 5, pp. 811–816, Apr. **2007**.
- [140] A. B. Zezin, V. B. Rogacheva, V. I. Feldman, P. Afanasiev, and A. A. Zezin, “From triple interpolyelectrolyte-metal complexes to polymer-metal nanocomposites,” *Adv. Colloid Interface Sci.*, vol. 158, no. 1–2, pp. 84–93, Jul. **2010**.
- [141] D. Mott, J. Galkowski, L. Wang, A. J. Luo, and C.-J. Zhong, “Synthesis of Size-Controlled and Shaped Copper Nanoparticles,” *Langmuir*, vol. 23, no. 10, pp. 5740–

5745, **2007**.

- [142] S. D. Sütekin and O. Güven, “Radiation-induced controlled polymerization of acrylic acid by RAFT and RAFT-MADIX methods in protic solvents,” *Radiat. Phys. Chem.*, vol. 142, pp. 82–87, Jan. **2018**.
- [143] S. P. Le-Masurier, G. Gody, S. Perrier, and A. M. Granville, “One-pot polymer brush synthesis via simultaneous isocyanate coupling chemistry and ‘grafting from’ RAFT polymerization,” *Polym. Chem.*, vol. 5, no. 8, pp. 2816–2823, Mar. **2014**.
- [144] I. Száraz and W. Forsling, “A spectroscopic study of the solvation of 1-vinyl-2-pyrrolidone and poly(1-vinyl-2-pyrrolidone) in different solvents,” *Polymer (Guildf)*, vol. 41, no. 13, pp. 4831–4839, Jun. **2000**.
- [145] Y. Liu, Q. Ma, X. Dong, W. Yu, J. Wang, and G. Liu, “A novel strategy to directly fabricate flexible hollow nanofibers with tunable luminescence–electricity–magnetism trifunctionality using one-pot electrospinning,” *Phys. Chem. Chem. Phys.*, vol. 17, no. 35, pp. 22977–22984, Aug. **2015**.
- [146] I. V. Korolkov *et al.*, “Electron/gamma radiation-induced synthesis and catalytic activity of gold nanoparticles supported on track-etched poly(ethylene terephthalate) membranes,” *Mater. Chem. Phys.*, vol. 217, pp. 31–39, Sep. **2018**.
- [147] S.-D. Oh *et al.*, “Dispersing of Ag, Pd, and Pt–Ru alloy nanoparticles on single-walled carbon nanotubes by γ -irradiation,” *Mater. Lett.*, vol. 59, no. 10, pp. 1121–1124, Apr. **2005**.
- [148] A. R. Anderson and E. J. Hart, “Radiation chemistry of water with pulsed high intensity electron beams,” *J. Phys. Chem.*, vol. 66, no. 1, pp. 70–75, Jan. **1962**.
- [149] G. R. Dey, “Reduction of the copper ion to its metal and clusters in alcoholic media: A radiation chemical study,” *Radiat. Phys. Chem.*, vol. 74, no. 3–4, pp. 172–184, Oct. **2005**.
- [150] J. V. Rojas and C. H. Castano, “Production of palladium nanoparticles supported on multiwalled carbon nanotubes by gamma irradiation,” *Radiat. Phys. Chem.*, vol. 81, no. 1, pp. 16–21, Jan. **2012**.
- [151] M. Rakap, “Poly(N-vinyl-2-pyrrolidone)-stabilized palladium platinum nanoparticles catalyzed hydrolysis of ammonia borane for hydrogen generation,” *J. Power Sources*, vol. 276, pp. 320–327, Feb. **2015**.

- [152] M. Mostafavi, G. R. Dey, A. L. François, and J. Belloni, “Transient and Stable Silver Clusters Induced by Radiolysis in Methanol,” *J. Mater. Chem. A*, vol. 106, no. 43, pp. 10184–10194, **2002**.
- [153] G. R. Dey and K. Kishore, “Silver clusters in 2-propanol: a radiation chemical study,” *Radiat. Phys. Chem.*, vol. 72, no. 5, pp. 565–573, Apr. **2005**.
- [154] C. Jonah and D. Bartels, “Radiolytically Induced Formation and Optical Absorption Spectra of Colloidal Silver Nanoparticles in Supercritical Ethane ,” *J. Phys. Chem. B*, vol. 105, no. 5, pp. 954–959, **2001**.
- [155] M. Sarmah, A. B. Neog, P. K. Boruah, M. R. Das, P. Bharali, and U. Bora, “Effect of Substrates on Catalytic Activity of Biogenic Palladium Nanoparticles in C–C Cross-Coupling Reactions,” *ACS Omega*, vol. 4, no. 2, pp. 3329–3340, Feb. **2019**.
- [156] P. A. Namini, A. A. Babaluo, and B. Bayati, “Palladium nanoparticles synthesis using polymeric matrix: poly(ethyleneglycol) molecular weight and palladium concentration effects,” *Int. J. Nanosci. Nanotechnol.*, vol. 3, no. 1, pp. 37–44, Dec. **2007**.
- [157] J. A. Johnson, J. J. Makis, K. A. Marvin, S. E. Rodenbusch, and K. J. Stevenson, “Size-Dependent Hydrogenation of *p*- Nitrophenol with Pd Nanoparticles Synthesized with Poly(amido)amine Dendrimer Templates,” *J. Phys. Chem. C*, vol. 117, no. 44, pp. 22644–22651, Nov. **2013**.
- [158] S. Singh, N. Kumar, M. Kumar, Jyoti, A. Agarwal, and B. Mizaikoff, “Electrochemical sensing and remediation of 4-nitrophenol using bio-synthesized copper oxide nanoparticles,” *Chem. Eng. J.*, vol. 313, pp. 283–292, Apr. **2017**.
- [159] Z. D. Pozun *et al.*, “A Systematic Investigation of *p* -Nitrophenol Reduction by Bimetallic Dendrimer Encapsulated Nanoparticles,” *J. Phys. Chem. C*, vol. 117, no. 15, pp. 7598–7604, Apr. **2013**.
- [160] P. Suchomel *et al.*, “Simple size-controlled synthesis of Au nanoparticles and their size-dependent catalytic activity,” *Sci. Rep.*, vol. 8, no. 1, p. 4589, Dec. **2018**.
- [161] Y. Yu, K. Kant, J. G. Shapter, J. Addai-Mensah, and D. Losic, “Gold nanotube membranes have catalytic properties,” *Microporous Mesoporous Mater.*, vol. 153, pp. 131–136, May **2012**.
- [162] C. A. Jaska *et al.*, “Poisoning of Heterogeneous, Late Transition Metal

Dehydrocoupling Catalysts by Boranes and Other Group 13 Hydrides,” *J. Am. Chem. Soc.*, vol. 127, **2005**.

- [163] M. Flytzani-Stephanopoulos, I. S. Nam, X. Verykios, H. Yamashita, R. W. McCabe, and G. L. Puma, “Applied Catalysis B: Environmental,” *Elsevier*, vol. 89, no. 1–2, pp. 104–110, **2009**.



HACETTEPE UNIVERSITY
GRADUATE SCHOOL OF SCIENCE AND ENGINEERING
THESIS/~~DISSERTATION~~ ORIGINALITY REPORT

HACETTEPE UNIVERSITY
GRADUATE SCHOOL OF SCIENCE AND ENGINEERING
TO THE DEPARTMENT OF POLYMER SCIENCE AND TECHNOLOGY

Date: 16/09/2019

Thesis Title / Topic: SYNTHESIS OF POLY(VINYLPYRROLIDONE) (PVP) GRAFTED SILICA AS MATRIX FOR GENERATION OF PALLADIUM NANOPARTICLES AND INVESTIGATION OF EFFECT OF GRAFT LENGTHS ON CATALYTIC ACTIVITY

According to the originality report obtained by myself/my thesis advisor by using the *Turnitin* plagiarism detection software and by applying the filtering options stated below on 13/09/2019 for the total of 71 pages including the a) Title Page, b) Introduction, c) Main Chapters, d) Conclusion sections of my thesis entitled as above, the similarity index of my thesis is 10 %.

Filtering options applied:

1. Bibliography/Works Cited excluded
2. Quotes ~~excluded~~ / included
3. Match size up to 5 words excluded

I declare that I have carefully read Hacettepe University Graduate School of Science and Engineering Guidelines for Obtaining and Using Thesis Originality Reports; that according to the maximum similarity index values specified in the Guidelines, my thesis does not include any form of plagiarism; that in any future detection of possible infringement of the regulations I accept all legal responsibility; and that all the information I have provided is correct to the best of my knowledge.

I respectfully submit this for approval.

Date and Signature

Name Surname: TANSU ÇAYLAN

Student No: N15128051

Department: POLYMER SCIENCE AND TECHNOLOGY

Program: -

Status: Masters Ph.D. Integrated Ph.D.

16.09.2019

ADVISOR APPROVAL

APPROVED.

Assoc. Prof. Dr. Murat Barsbay

(Title, Name Surname, Signature)

CURRICULUM VITAE

Name, Surname : Tansu ÇAYLAN
Place of Birth : Ankara
Date of Birth : 29.05.1992
Material Status : Married
Tel : 05304082678
E-mail : tansu.caylan92@gmail.com
Foreign Language : English, Good

Education

BSc : Department of Chemical Engineering- Middle East
Technical University, Ankara (Turkey), GPA: 2.56 / 4.00
MSc. : Department of Polymer Science and Technology- Hacettepe
University, Ankara (Turkey), GPA: 3.58 / 4.00

Work Experience

2019-working : Roketsan A.Ş.
2017- 2019 : Turkish Standards Institution (TSE)
Aug 2014-Sept 2014 : Intern
Turkish Aerospace Industries (TAI), Kazan /ANKARA
Aug 2013- Sept 2013 : Intern
BAŞTAŞ Cement Ins. Elmadağ /ANKARA
Computer Skills : MS Windows, FORTRAN, Aspen PLUS, MATHCAD,
MATHLAB, OriginPro 8.5, ChemDraw Ultra 12

Other Skills

Project

- 2014 Processes of Ethylene Oxide Gas Production (Ch.E.-METU)

This project was about the production ethylene oxide. The reactors used in the production process of ethylene oxide were designed.

- 2014 Ethylene Oxide Productions by Direct Oxidation (Ch.E.-METU)
- 2015 Separation of Ethylene Oxide (Ch.E.-METU)
- 2015 Ethylene Oxide Production Plant Design (Ch.E.-METU)
- 2015 Composite Materials used in Aircrafts (METE-METU)

Presentations

- Poster Presentation of Ethylene Oxide Production Plant Design, Gazi University Ankara, Turkey
- Poster Presentation of Ethylene Oxide Production Plant Design, Ch.E. - METU, Ankara, Turkey

Seminars

22-23 October 2014 : Somer Lectures by Prof. Dr. Mark-Olivier Coppens, 'A Chemical Engineering Approach To Addressing Global Challenges'

20 March 2015 : Prof. Dr. Göknur BAYRAM 'Polymers with Composite Materials

2-5 March 2015 : ODTÜ, KKM METU Career Days (Kampüs Gelişim Günleri)

Areas of experience

Technical : Reactor design and chemical engineering process, engineering economics, fluid mechanics, composite materials, polymer science and technology, polymerization techniques and synthesis

